

AD-A181 990

# NAVAL POSTGRADUATE SCHOOL

Monterey, California

DTIC FILE COPY



DTIC  
ELECTE  
JUL 09 1987  
S D

## THESIS

A COMPARISON OF THE AN/GMD-1 RAWINSONDE  
WITH  
THE AN/TPQ-37 RADAR (WINDFINDER)  
AS THEY AFFECT BALLISTIC ARTILLERY

by

Gary L. Stipe

March 1987

Thesis Advisor E. B. Rockower

Approved for public release; distribution is unlimited.

REPORT DOCUMENTATION PAGE

1a REPORT SECURITY CLASSIFICATION <b>UNCLASSIFIED</b>		1b RESTRICTIVE MARKINGS	
2a SECURITY CLASSIFICATION AUTHORITY		3 DISTRIBUTION/AVAILABILITY OF REPORT Approved for public release; distribution is unlimited	
2b DECLASSIFICATION/DOWNGRADING SCHEDULE			
4 PERFORMING ORGANIZATION REPORT NUMBER(S)		5 MONITORING ORGANIZATION REPORT NUMBER(S)	
6a NAME OF PERFORMING ORGANIZATION <b>NAVAL POSTGRADUATE SCHOOL</b>	6b OFFICE SYMBOL (if applicable) <b>55</b>	7a NAME OF MONITORING ORGANIZATION <b>NAVAL POSTGRADUATE SCHOOL</b>	
6c ADDRESS (City, State, and ZIP Code) <b>Monterey, California 93943-5000</b>		7c ADDRESS (City, State, and ZIP Code) <b>Monterey, California 93943-5000</b>	
8a NAME OF FUNDING/SPONSORING ORGANIZATION	8b OFFICE SYMBOL (if applicable)	9 PROCUREMENT INSTRUMENT IDENTIFICATION NUMBER	
8c ADDRESS (City, State, and ZIP Code)		10 SOURCE OF FUNDING NUMBERS	
		PROGRAM ELEMENT NO	PROJECT NO
		TASK NO	WORK UNIT ACCESSION NO
11 TITLE (Include Security Classification) <b>A COMPARISON OF THE AN/GMD-1 RAWINSONDE WITH THE AN/TPQ-37 RADAR (WINDFINDER) AS THEY AFFECT BALLISTIC ARTILLERY</b>			
12 PERSONAL AUTHOR(S) <b>STIPE, Gary L.</b>			
13a TYPE OF REPORT <b>Master's Thesis</b>	13b TIME COVERED FROM _____ TO _____	14 DATE OF REPORT (Year, Month, Day) <b>1987 March</b>	15 PAGE COUNT <b>58</b>
16 SUPPLEMENTARY NOTATION			
17 COSATI CODES		18 SUBJECT TERMS (Continue on reverse if necessary and identify by block number)	
FIELD	GROUP	SUB-GROUP	
		Radar, Meteorology, Ballistics, Firing Theory, Artillery, Firefinder, Wind Profiles, Windfinder	
19 ABSTRACT (Continue on reverse if necessary and identify by block number)			
<p>This thesis is an examination of using a fielded doppler shift radar, specifically the AN/TPQ-37 (FIREFINDER), to gather wind signature data for use in ballistic artillery calculations. Stale rawinsonde data and current radar gathered data are compared to current rawinsonde data as they affect the artillery probability of kill P(k) against a point target. Graphical results as well as parametric and non-parametric tests are used to determine any statistical differences in the results of the tests. Final recommendations include continued research, as well as a physical test firing to compare the accuracy of the two systems.</p>			
20 DISTRIBUTION/AVAILABILITY OF ABSTRACT <input checked="" type="checkbox"/> UNCLASSIFIED/UNLIMITED <input type="checkbox"/> SAME AS RPT <input type="checkbox"/> DTIC USERS		21 ABSTRACT SECURITY CLASSIFICATION	
22a NAME OF RESPONSIBLE INDIVIDUAL <b>E. B. Rockower</b>		22b TELEPHONE (Include Area Code) <b>408-646-2191</b>	22c OFFICE SYMBOL <b>55Rf</b>

*C. necessary include*

Approved for public release; distribution is unlimited.

**A Comparison of the AN/GMD-1 Rawinsonde with  
the AN/TPQ-37 Radar (WINDFINDER)  
As They Affect Ballistic Artillery**

by

**Gary L. Stipe  
Major, United States Army  
B.S.E.E., Montana State University, 1975**

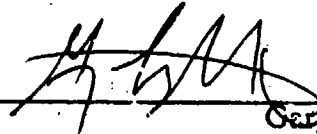
Submitted in partial fulfillment of the  
requirements for the degree of

**MASTER OF SCIENCE IN OPERATIONS RESEARCH**

from the

**NAVAL POSTGRADUATE SCHOOL  
March 1987**

Author:

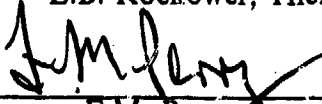


Gary L. Stipe

Approved by:



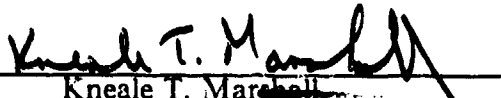
E.B. Rockower, Thesis Advisor



F.M. Perry, Second Reader



P. Purdue, Chairman,  
Department of Operations Research



Kneale T. Marshall  
Dean of Information and Policy Science

## ABSTRACT

This thesis is an examination of using a fielded doppler shift radar, specifically the AN/TPQ-37 (FIREFINDER), to gather wind signature data for use in ballistic artillery calculations. Stale rawinsonde data and current radar gathered data are compared to current rawinsonde data as they affect the artillery probability of kill  $P(k)$  against a point target. Graphical results as well as parametric and non-parametric tests are used to determine any statistical differences in the results of the tests. Final recommendations include continued research, as well as a physical test firing to compare the accuracy of the two systems.

Accession For	
NTIS CRA&I	<input checked="" type="checkbox"/>
DTIC TAB	<input type="checkbox"/>
Unannounced	<input type="checkbox"/>
Justification .....	
By .....	
Distribution /	
Availability Codes	
Dist	Avail and/or Special
A-1	



## TABLE OF CONTENTS

I.	INTRODUCTION .....	9
	A. EXECUTIVE SUMMARY .....	9
	1. Background .....	9
	2. Objective .....	13
	3. Data .....	13
	4. Problem .....	14
	5. Model .....	14
	6. MOE .....	15
	7. Analysis .....	16
	8. Conclusions and Recommendations .....	17
	B. THESIS OUTLINE .....	17
II.	DATA PREPARATION .....	19
	A. GTRAJ .....	19
	B. GENERATION PROCESS .....	20
	C. REFERENCE ORIGIN .....	22
III.	MODEL DEVELOPMENT .....	25
	A. MODEL .....	25
	B. BIAS DETERMINATION .....	26
IV.	MOE DETERMINATION .....	30
	A. ALTERNATIVES .....	30
	B. CALCULATION OF MOE .....	30
V.	CALCULATION OF P(K) .....	32
	A. DAMAGE FUNCTION .....	32
	1. Cookie cutter .....	33
	2. Diffuse Gaussian .....	33
	B. FIRING DISTRIBUTION .....	34

C.	DETERMINATION OF P(K) .....	34
1.	Numerical Determination .....	34
2.	Graphical Determination .....	35
VI.	ANALYSIS OF RESULTS .....	39
A.	GRAPHICAL ANALYSIS .....	39
B.	STATISTICAL TESTING .....	40
VII.	CONCLUSIONS AND RECOMMENDATIONS .....	50
A.	CONCLUSIONS .....	50
B.	RECOMMENDATIONS .....	50
APPENDIX A:	COMPUTER MET MESSAGES .....	51
APPENDIX B:	INDIVIDUAL RANGE P(K) RESULTS .....	53
LIST OF REFERENCES	.....	55
INITIAL DISTRIBUTION LIST	.....	57

## LIST OF TABLES

1. MET DATA COMPARISONS .....	17
2. GTRAJ INPUT VALUES .....	22
3. BALLOON BIAS VS RANGE TO TARGET .....	28
4. BALLISTIC DISPERSION ESTIMATES FOR 155MM HOWITZER, M109A1 .....	28
5. TARGET RANGE DISTRIBUTION .....	31
6. BALLISTIC DISPERSION ESTIMATES FOR 155MM HOWITZER, M109A1 .....	34
7. MET COMPARISON P(K) .....	37
8. GOODNESS OF FIT TEST SIGNIFICANCE LEVELS .....	40
9. CALCULATED P(K) FOR MET COMPARISONS .....	47
10. TWO SAMPLE t TEST RESULTS .....	48
11. MANN-WHITNEY TEST RESULTS .....	49

## LIST OF FIGURES

1.1	Radar Wind Profiling .....	12
1.2	Target Location Model .....	15
2.1	Data Generation Flow-chart .....	21
2.2	Transformation to Reference Origin .....	24
3.1	Target Location Model .....	26
5.1	Graphical Bias Determination .....	36
6.1	Histograms of Radar $P(k)$ .....	41
6.2	Histograms of Two Hour Balloon $P(k)$ .....	42
6.3	Histograms of Four Hour Balloon $P(k)$ .....	43
6.4	Q - Q Plots Radar $P(k)$ Quantiles vs Two Hour $P(k)$ Quantiles .....	44
6.5	Q - Q Plots Radar $P(k)$ Quantiles vs Four Hour $P(k)$ Quantiles .....	45



## ACKNOWLEDGEMENTS

As the author, I would like to express my sincere appreciation to the following individuals, for without their timely and generous assistance, this thesis could not have been produced: My second reader LTC F. Marchman Perry, my points of contact at the Atmospheric Sciences Laboratory, Dr. D. Snider, Dr. J. Martin and Mr. A. Blanco, and classmates MAJ David Tyner and LCDR J. William "Pops" Goodwin.

My thesis advisor Professor Edward B. Rockower, deserves not only my sincere thanks for the guidance and assistance in the analysis, but thanks also for providing the key insights necessary to develop the analytical model and the graphical analysis technique. He has made this a learning experience that was both rewarding and enjoyable.

Lastly, I want to thank my wife Beverly, lovingly referred to as "SAM." As a career Army Officer, she put up with this two and a half year geographical separation, and excelled in her career, yet always provided the love, support, and understanding necessary to keep me going.

To all of you, my heart-felt thanks.

## I. INTRODUCTION

Meteorology data is used by all branches of the service to aid in performance of some portion of their operational mission. This information is used by the artillery and air defense artillery for ballistic calculations. It is used by chemical personnel to provide accurate down wind predictions for chemical and nuclear contaminants. The aviation industry has been searching for ways to more accurately depict the current wind profiles (wind speed and direction at various altitudes) around major airports to reduce the number of severe wind related accidents. The National Oceanic and Atmospheric Administration (NOAA) has conducted numerous tests and extensive experimentation [Refs. 1,2: pp. 48,25], where they conclude that radar can be used to measure the wind profiles in certain atmospheric conditions. NOAA has also concluded that the U.S. Army's AN/TPQ-37 (FIREFINDER), an X-band radar, can provide wind profiles in the presence of precipitation, and at cloud heights, but can not furnish wind measurements routinely up to 8 - 10 km in the optically clear atmosphere due to it's short wavelength [Ref. 3: p. 3]. Chapter I begins with an Executive Summary, which outlines the problem, the solution approach, the analysis, and conclusions. Chapter I concludes with an overall outline of the thesis.

### A. EXECUTIVE SUMMARY

#### 1. Background

##### *a. Current Concerns*

Having accurate and timely meteorological data is very important today if the probability of a first round hit on a target of known location by field artillery is to be improved. There are many factors that affect the accuracy of an artillery weapon. The age of the tube (demonstrated by the internal wear and overall effects of metal fatigue), the human errors that occur when aiming the tube (both in azimuth and elevation), and survey errors which occur when establishing the location of the gun are just a few of the non-meteorologically induced errors which affect the point of impact of the rounds.

In the field artillery, ballistic meteorology is concerned with determining atmospheric conditions in the area where artillery rounds or rockets will be fired. Atmospheric conditions along the trajectory of a projectile directly affect its accuracy

and may cause it to miss the desired point of impact. The meteorologically imposed error can be as much as 5 to 10 percent of the range, even under stable weather conditions [Ref. 4: p. 2-1]

In the U.S. Army, meteorological (MET) data is used when computing the trajectories of artillery and mortar rounds, and when adjusting friendly fires. MET data is also used by sound ranging platoons in determining enemy artillery locations and by the chemical personnel when predicting the effects of the atmosphere on chemical radiological contaminants that may be introduced in the course of battle.

For all of these uses, it is imperative that the data be as current and as accurate as is physically and technically possible.

***b. Current System***

Currently, the U.S. Army relies on the Meteorological Section assigned to the division artillery to gather, analyze, and distribute the necessary data. To do this, the MET section periodically flies weather balloons. The balloons carry a radiosonde instrument package which directly measures air temperature, humidity and barometric pressure. This data is continuously transmitted to a ground station which tracks the balloon as it rises through the atmosphere. The tracking data thereby provides wind speed and direction at the various altitudes (or zones) necessary for ballistic calculations using standard trigonometric and analytic geometry techniques. This data is analyzed and collated by the MET section and then sent via secure radio-teletype to an operator located at the artillery battalion fire direction center (FDC) where it is entered into the tactical fire direction system (TACFIRE) computer by hand. Henceforth, this data will be referred to as balloon MET data. This data is then used for all artillery firing calculations until the next meteorological data update. By doctrine, this is supposed to occur every four hours; however, in combat, where units are constantly on the move, it is very doubtful that the update will occur that often. A more realistic figure might be every six hours. This allows for the movement of the MET station, equipment setup, balloon preparation and flight, data analysis, and transmission of the data to the FDC.

This large time lag in data updates could potentially cause large errors in the accuracy of artillery fire missions. Due to the dynamics of the atmosphere, this can happen in as little as two hours [Ref. 5], and in less time if a storm front moves through the area during that time, since more error is introduced into the data in these situations.

*c. Radar MET*

The requirement then is to update the MET data in a timely manner to ensure reasonable accuracy in artillery fire missions. One alternative is to accept the error and make the best of the system that is currently fielded. This should be considered as a baseline situation from which any improvement can be measured.

Another alternative would be to double or triple the number of MET sections, thereby allowing for staggered balloon flights, accomplishing an update every two hours or so. The expense in both manpower and equipment quickly gets very large with this alternative.

A third alternative involves using a different system for obtaining MET data. One such system is a doppler shift radar with a phased array antenna which can provide the necessary wind profile when used in conjunction with a mathematical algorithm. [Ref. 6], developed at the U.S. Army Atmospheric Sciences Laboratory (ASL) for predicting temperature and barometric pressure at the various altitudes of the wind profile based on values obtained on the ground. The latter is known as an "analytic atmosphere." The radar can be used as follows; at each altitude, the radar samples the atmosphere in two directions, see Figure 1.1. The angle between the radar sampling beams should be about 70 - 90 degrees. Lower separation angles have been used but they did not appear to produce as accurate a wind profile [Ref. 3: p. 17]. After all altitudes have been sampled, signal processing techniques are employed to extract the wind profile. Currently this signal processing is performed off-line from the radar, but software to accomplish real-time processing of the wind profile is being developed through efforts at ASL.

The "analytic atmosphere" is based on the current time of day, current surface readings of temperature and barometric pressure, and the minimum and maximum temperature readings from the previous day. It provides temperature and barometric pressure values at twenty-six altitudes which are then stored in a computer file along with the wind profile provided by the FIREFINDER radar to produce a computer MET message in a special format for input to the TACFIRE computer. Currently, this data is entered by hand, but because of the nature of the radar and the existence of communications links between the TACFIRE computer and the radar, the potential for automated MET data updating from the radar to the TACFIRE computer exists. The project at ASL to incorporate wind profiling into FIREFINDER capabilities along with the analytic atmosphere is known as WINDFINDER.

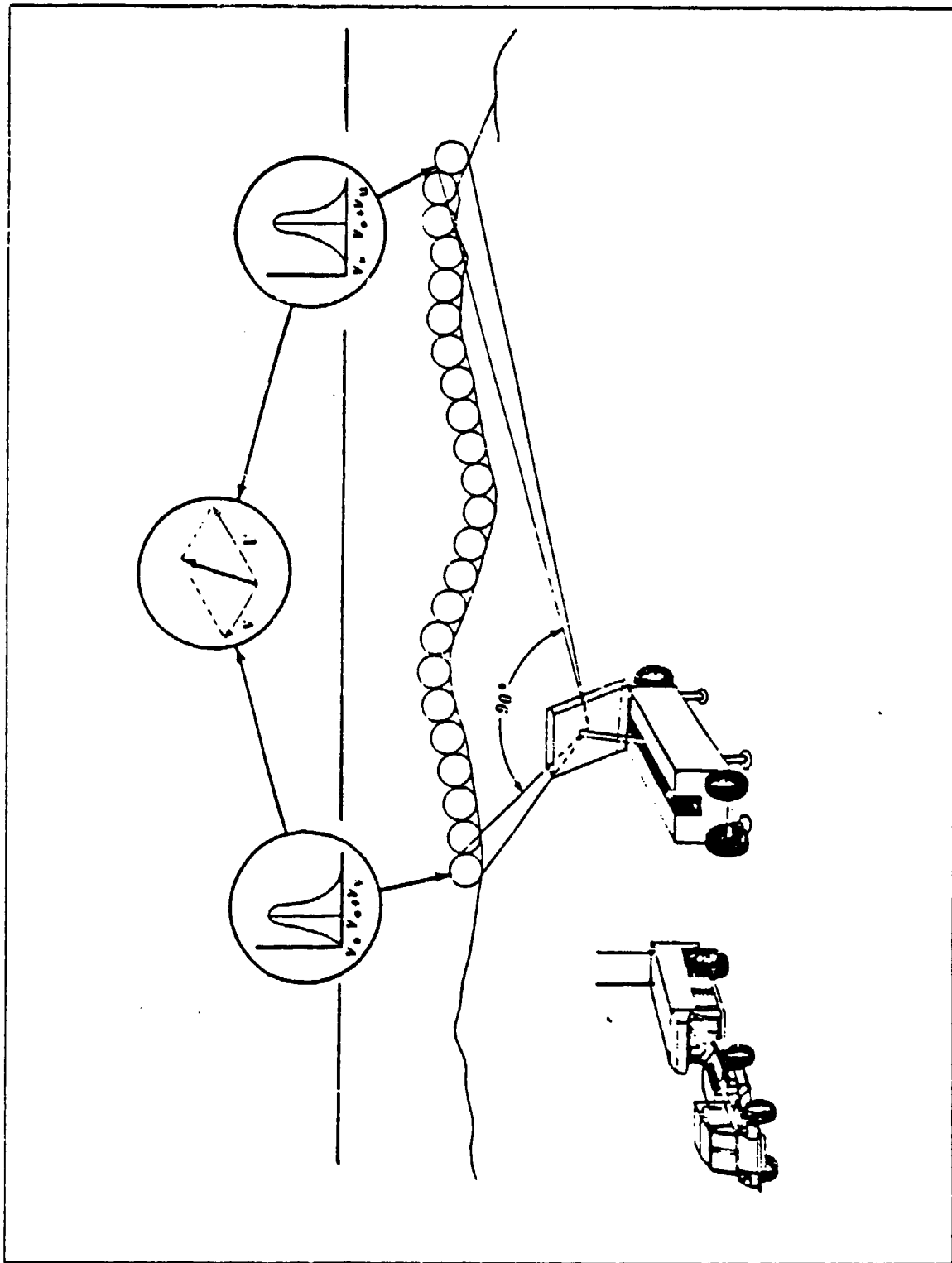


Figure 1.1 Radar Wind Profiling.

NOAA has concluded that the FIREFINDER radar can sense wind profiles on a limited basis. Whether the MET data provided by WINDFINDER is accurate enough for ballistic artillery has not been determined.

## **2. Objective**

In late 1987, the US Army will start fielding an improved meteorological data gathering system known as the MET Data System, (MDS), AN/TMQ-31. This system is reported to be a vastly improved radiosonde system, that incorporates automatic data transmission to TACFIRE. The current fielding plan indicates that two MDS will be fielded at each of the infantry and armor divisions in the US Army. Field artillery brigades, and separate infantry and armor brigades are to receive one MDS each. The US Army Field Artillery School at Ft. Sill, OK will receive eight systems for testing and training, and other systems will go into war reserves. In all, fifty-five MDS are to be procured at an estimated cost of \$1.5 million each. An additional seven downsized systems are to be procured for the light infantry divisions, the 82nd ABN Division, and the 101st ABN (Air Assault) Division.

This thesis is a pilot study whose objective is to determine, using the limited data available, if the FIREFINDER radar, operating in the WINDFINDER mode, can successfully augment the current balloon MET to provide data to the TACFIRE computer for ballistic artillery fire missions as a low cost alternative to the almost \$100 million MDS system upgrade.

## **3. Data**

Ideally, the way to compare two MET systems is to fire rounds under a wide range of conditions using each system (radar & balloon) and compare the accuracy of the results. Unfortunately, because of limited funds no actual firings have been conducted.

During the period 28 February 1986 - 8 March 1986, ASL gathered MET data at Yuma Proving Grounds, AZ. The data consisted of balloon MET and concurrent radar MET. The MET station at Yuma normally flies a balloon at 0500hrs, 0800hrs, 1000hrs, 1200hrs and 1400hrs, unless funded projects have coordinated a change in that schedule. Due to a shortage of funds, the decision was made at ASL to gather radar MET data in conjunction with just the normal balloon schedule at Yuma. The results of the experiment were 19 balloon MET and radar MET data sets. Appendix A contains the first balloon MET and radar MET data sets in the format of a computer MET message.

#### 4. Problem

The only analytical tool readily available to perform ballistic artillery calculations as a function of meteorology input [Ref. 7], was a computer model developed at the US Army Ballistic Research Laboratory (BRL), Aberdeen Proving Grounds, Maryland. One of the weaknesses of this model for the purposes of this thesis was its deterministic nature. If a target was specified, then the model would provide a quadrant elevation and initial deflection for the gun to "hit the target." Conversely, a quadrant elevation and initial deflection could be specified and the model would indicate the location of the target at which the gun was "aiming." So, using the model, there was no direct way to compare the two MET data sets. However, if the model were used to determine the quadrant elevation and initial deflection using one MET data set (assuming that the aim point was the actual target), then switching operating modes, the other MET data set could be used to determine a second "aim point" based on the previously determined quadrant elevation and deflection. The distance between this aim point and the target location would then provide a measure of the relative accuracy of the second data set to the first. The model was then used with the balloon MET data set as the reference data set. The next problem was to determine the absolute accuracy of the radar data using only the relative-to-balloon data that was generated using the BRL model.

#### 5. Model

FM 6-141-1 [Ref. 8: p. 5-6], specifies the probability of hitting,  $P(h)$ , a target 20 meters by 20 meters for various ranges. Using those values, it was a simple matter to determine the absolute accuracy of the balloon MET data that was necessary to produce the listed  $P(h)$  for each range.

Having the absolute accuracy for the balloon MET data, and the relative-to-balloon accuracy for the radar MET data, a model was required that described the interaction of those two parameters that would yield an estimate of the absolute accuracy of the radar MET data.

If we assume that the target location (T) is known, then we can compare the two MET systems by comparing the results of using each system. Figure 1.2 shows the relative positions of the target and the two aim points. If the balloon MET is used, an aim point is produced. Ideally, this aim point should be located at T. However, the balloon MET system is not 100% accurate, so a random bias exists from T to the balloon MET aim point B. This also applies to the radar MET system and its aim

point R. The difference between T and B is a random vector. Call it  $TB$ . Likewise, from T to R is a random vector  $TR$ . The difference of these two random vectors  $TB - TR$  is another random vector  $RB$ .  $RB$  is the relative bias between the balloon MET and the radar MET and is included in the data generated by the BRL model, by virtue of using the balloon MET as a reference standard.

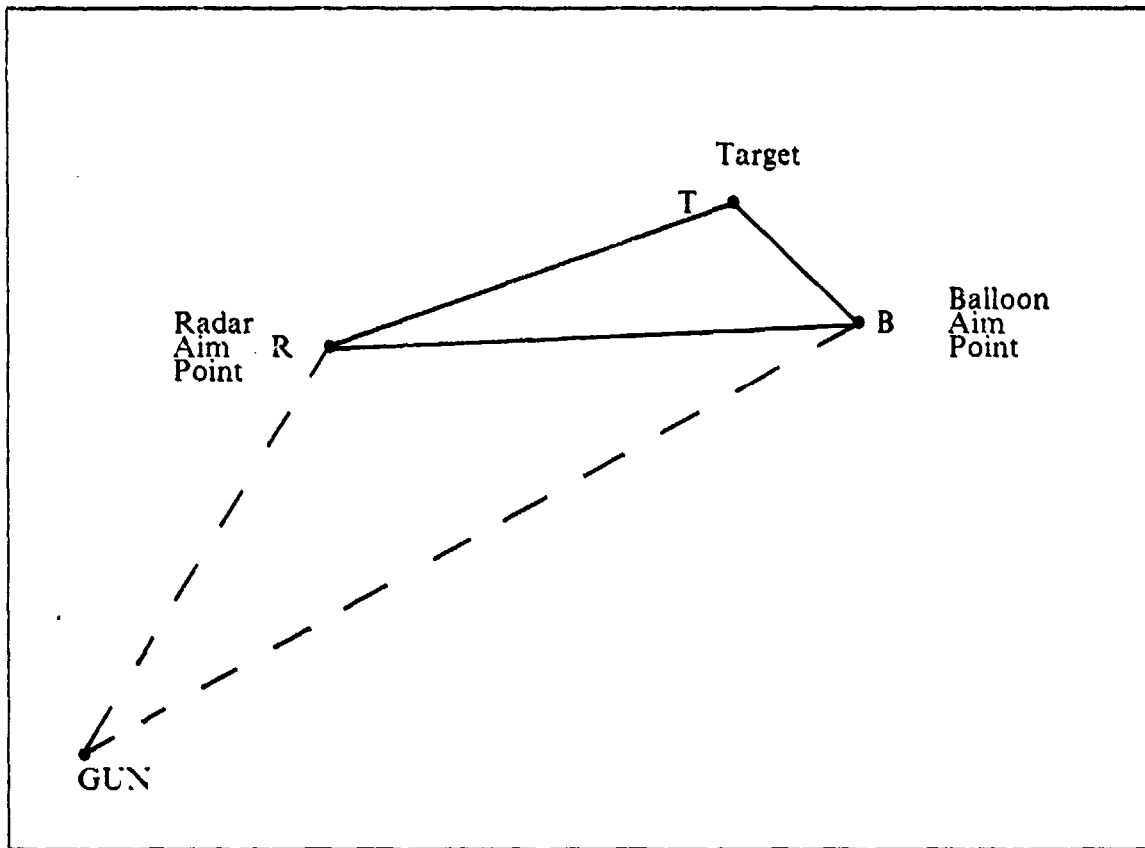


Figure 1.2 Target Location Model.

## 6. MOE

In any analytical effort where a decision must be made between two or more alternatives, some measure of effectiveness (MOE) must be used to keep the choice from being subjective, emotionally motivated and unsupportable in the face of test data and evaluations. Rockower [Ref. 9: p. 3], specifies that "a crucial part of the initial analysis is selection of the appropriate *measure of effectiveness*." This MOE facilitates an objective, normally numerically valued, comparison between the alternatives. Since this was an analysis of the effect produced by two different MET data systems on



ballistic artillery. the probability of kill,  $P(k)$ , produced by each system was chosen as the MOE.

### 7. Analysis

To represent the fact that targets are found at different ranges from the gun, three different ranges were used in the analysis. To eliminate any regional effects from prevailing winds, the  $P(k)$  was calculated for eight different directions of fire for each of the three ranges. These  $P(k)$ 's were then averaged to produce an average  $P(k)$  for the range distribution chosen. Based upon conversations with numerous US Army and US Marine Corps artillery officers at Ft. Ord, CA, Ft. Sill, OK, and the Naval Postgraduate School, Monterey, CA, three ranges, 10km, 12km, and 14km, were chosen as "realistic" ranges for which a 155mm howitzer would be employed. Two range distributions were considered, one where the target was assumed to be equally likely at any one of the three ranges, and a second distribution where the target was assumed to be at 12km half of the time, and a quarter of the time at 10km or 14km. These range distributions are purely subjective, and do not reflect any "expected," or doctrinal distributions.

The objective was to determine if the radar MET could augment the balloon MET, not replace it. Because the much lower cost of the radar's software development compared with the alternative of procuring additional balloon MDS units was sufficient reason to choose the radar, so long as using the radar resulted in performance *no worse than* the alternative, the hypothesis to be tested was:

$H_0$ : Radar MET is at least as good as stale balloon MET

with an alternative of:

$H_1$ : Radar MET is not as good as stale balloon MET

This translates into numerical symbology as:

$H_0$ : Radar MET  $P(k) \geq$  stale balloon MET  $P(k)$

$H_1$ : Radar MET  $P(k) <$  stale balloon MET  $P(k)$

There were 44 comparisons made for the analysis, see Table 1. Because of the limited data, many of the comparisons have only a few data points, as indicated. All comparisons were made using the current balloon MET as the reference data set to provide quadrant elevation and deflection.

**TABLE 1**  
**MET DATA COMPARISONS**

Comparisons	Data Points
Current radar	19
2hr old balloon	9
3hr old balloon	3
4hr old balloon	5
5hr old balloon	2
6hr old balloon	2
7hr old balloon	2
9hr old balloon	2

It was found that in all comparisons, with a level of significance of  $\alpha = .05$ , the alternative hypothesis ( $H_1$ ) could not be accepted.

### 8. Conclusions and Recommendations

Since the original data was so sparse and not gathered with this analysis in mind, results are not as conclusive as a properly designed experiment could show. Based upon the results, it can not be concluded that the radar MET is worse than the stale balloon MET. The large level of significance required to reject the hypothesis that the radar MET was as good as the balloon MET indicates the  $P(k)$  provided by the radar MET was statistically as good as that provided by the balloon MET. As such, the conclusion that the radar MET can be used to augment the balloon system is very strongly supported.

Given such strong indications of parity between the two MET systems, the next phase of testing should be pursued. These results warrant the expense of a field test where both MET systems are employed and targets are engaged with artillery of all calibers. The test should employ the balloon in its doctrinal operational mode, and the radar should be employed every two hours. The guns should fire under the same target conditions and should employ the MET data available at that time. The comparison in this case must be of the actual miss distance from the target to the point of impact.

### B. THESIS OUTLINE

The outline for the remainder of this thesis is basically the same as that used for the Executive Summary. The areas summarized above are discussed in much greater

depth in the respective chapters. In Chapter II, the data gathering and preparation is described in more detail. Following that, Chapter III presents a development of the analytic model. Chapter IV discusses the selection and calculation of the MOE, while the calculations necessary to determine the  $P(k)$  are developed in Chapter V. Chapter VI presents the analysis of the results of the two range distributions. Chapter VII contains the final conclusions and recommendations. Appendix A contains an example of the balloon MET and radar MET data sets. Appendix B has values for the results of each individual range.

## II. DATA PREPARATION

The original MET data was collected at Yuma Proving Grounds, AZ by ASL, as described in Chapter I. Due to the sparseness of the data, a method of comparing the effects of the radar MET data against the balloon MET data had to be devised. The only analytical tool to compare MET effects on artillery fires which was readily available and accepted throughout the artillery and ballistic meteorology communities [Ref. 7] was the General Trajectory Program (GTRAJ) written by the US Army Ballistic Research Laboratory, Aberdeen Proving Grounds, MD.

### A. GTRAJ

The General Trajectory Program was developed to assist in the development of artillery ammunition, propellants, and related products [Ref. 10]. It is written in FORTRAN 77 and installed on a DEC PDP 11/780 (VAX) series computer. It uses the point mass or modified point mass trajectory model to compute trajectories for boosted and non-boosted projectiles [Ref. 11]. As such, the model is completely deterministic and does not incorporate ballistic dispersion in its output [Ref. 12]. Washburn [Ref. 13: p. 1], describes ballistic dispersion as a probability density function for firing errors which incorporates the round to round variation in both cross-range and down-range impact point values. Since no ballistic dispersion is assumed, the output from GTRAJ is where the gun was "aimed," given the initial conditions assumed and the MET data base in use at the time [Ref. 11]. This determines the aim bias. It is this aim point that will be used to calculate a  $P(k)$  after incorporating ballistic dispersion into the analysis.

GTRAJ is a fully menu driven program that can be operated either interactively or from a batch file. It has many different integration modes that may be specified [Ref. 11]. The two used for this analysis are 1) integrate backward from a target of known location to determine the necessary quadrant elevation and deflection to aim directly at the target, and 2) given a quadrant elevation and deflection, integrate forward to determine the perceived aim point. Using this model, there was no way to directly evaluate the independent effects of both MET data sets. However, if the model was used with one MET data set to determine the quadrant elevation and initial deflection necessary to aim at a known target, then switched to the other operating

mode, the other MET data set could be used to determine a perceived aim point using the previously determined quadrant elevation and deflection. This aim point would not, in most cases, be the same as the originally chosen target location. This aim point would then provide a relative accuracy of the second MET data set compared to the first. The current balloon MET data set was always used in conjunction with the first mode of operation to determine the quadrant elevation and deflection necessary to aim the gun at the target. Using this output with the corresponding comparison MET data set, the second mode was used to determine the corresponding aim point.

## **B. GENERATION PROCESS**

A copy of GTRAJ was provided by ASL and installed on a DEC PDP 11/780 (VAX) located in the Computer Science Department at the Naval Postgraduate School, Monterey, CA.

The generation process is depicted at Figure 2.1. The model must be initialized by specifying the weapon system, ammunition type, mode of input (interactive or batch), and output file name. Next, the initial conditions are selected, the azimuth is set to 0.0 mils, and the mode of operation is set to integrate backward to determine the quadrant elevation and deflection for the given range. The balloon MET data file is specified and the computational parameters are set. This initial output produced is a quadrant elevation and deflection. Next, the operating mode is changed to integrate forward, the radar MET data file is specified, and the quadrant elevation and deflection just calculated are input. Keeping all other input parameters the same, GTRAJ is run again. This output is a range and deflection which is the perceived aim point for the radar MET in relation to the aim point of the balloon MET (target location). This point is stored in a separate data file for further processing. The next step is to increment the azimuth of fire by 800 mils ( $45^\circ$ ). The balloon MET data file is again specified, operational mode 1 (integrate backward) is selected and the process starts over again to generate another radar MET aim point. This process continues until aim points have been generated for the eight directions (N,NE,E,etc) for each of the three ranges, 10km, 12km, and 14km. All comparisons were made using the current balloon MET as the reference data set to provide quadrant elevation and deflection. The inputs that are required by GTRAJ [Ref. 11], and the values used for this analysis are in Table 2.

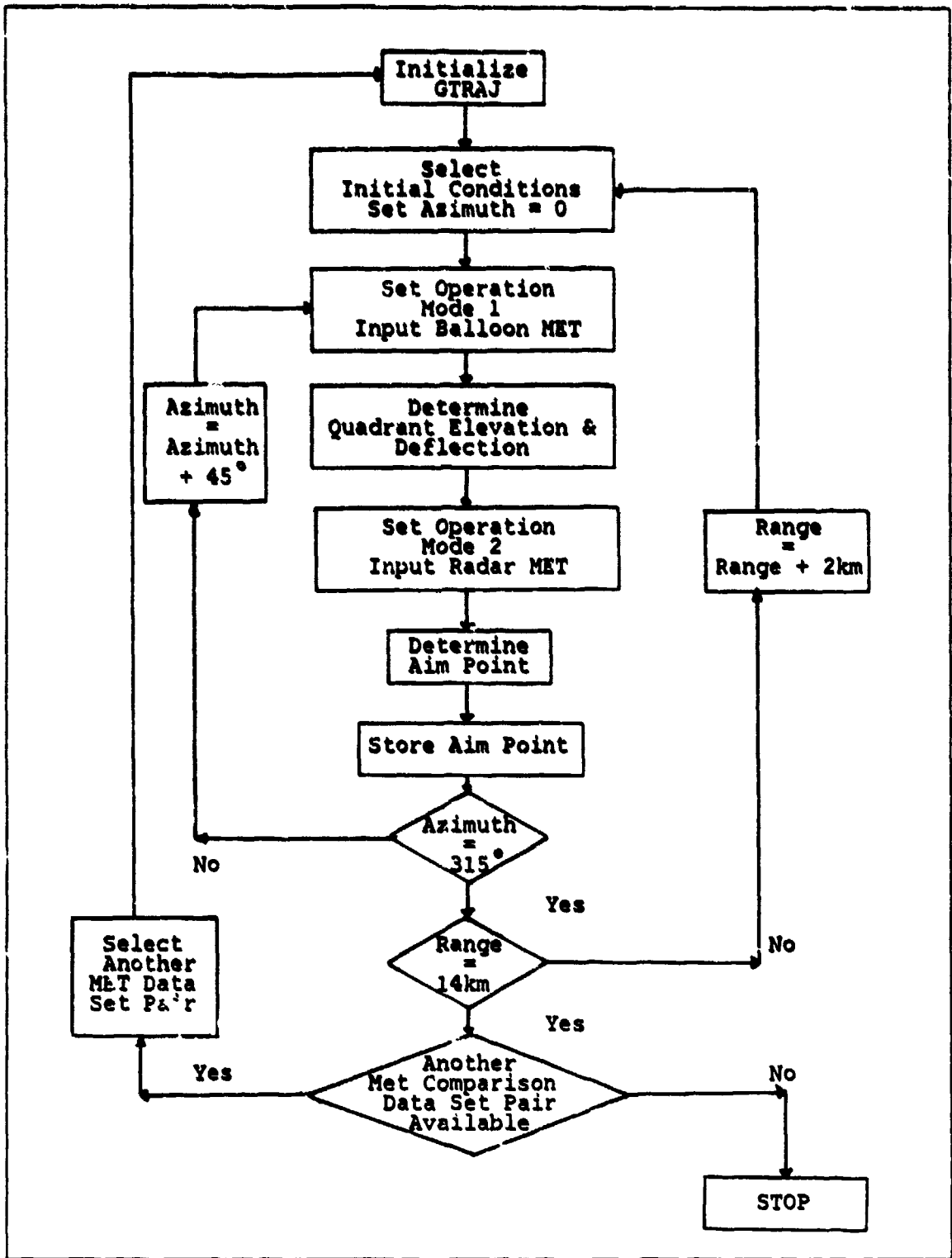


Figure 2.1 Data Generation Flow-chart.

**TABLE 2**  
**GTRAJ INPUT VALUES**

Required Input	Value Used
<b>Initialization</b>	
Weapon Caliber	155mm
Weapon system	M109A1
Ammunition	M107 - HE
<b>Initial conditions</b>	
Azimuth of fire	Variable
Curved earth or flat	Curved
Location of gun (X,Y,Z)	0,0,0
Location of target	Variable, Variable, 0
Range to target	10km, 12km, 14km
Mode of operation	Integrate from target to gun Integrate from gun to target
<b>Computational parameters</b>	
Charge	7W
Muzzle Velocity	568m/s
Powder Temperature	70° F
Quadrant Elevation	Variable
Deflection	Variable
Weight of round	95lbs
MET data file	Variable

**C. REFERENCE ORIGIN**

The output from GTRAJ is in the form of a range from the gun to the point of aim and a deflection, (D), which is a distance left (-) or right (+) of, and perpendicular to, the gun - target line. To know the exact point of aim, it is necessary to also know the direction of fire. To facilitate automated calculation of P(k), this aim point was

converted to an X,Y coordinate using the target location as the origin. In this manner, the dependence upon the direction of fire was removed. A standard translation of axis, as mentioned in Thomas, [Ref. 14: p. 518], was used to transform this original aim point, which was a function of range to the target and direction of fire, to an X,Y coordinate independent of the direction of fire. The conversion to the reference origin involves three phases. Referring to Figure 2.2, locate the target in the firing plane where the gun is assumed to be at the origin. The target is located at the point  $(X_1, Y_1)$ . This is a standard polar to rectangular coordinate conversion process, where  $R_1$  is the range to the target from the gun, and  $\theta$  is the direction of fire in degrees, using the standard rectangular coordinate system where the abscissa is associated with  $0^\circ$ .

$$X_1 = R_1 \cdot \cos\theta$$

$$Y_1 = R_1 \cdot \sin\theta$$

Next, the aim point must be located in this plane relative to the origin. The point  $(X_2, Y_2)$  is the location of the aim point, where  $R_2$  is the distance from the gun to the aim point, and  $D$ , the deflection, is the perpendicular distance left (-) or right (+) of the gun - target line.

$$X_2 = \sqrt{(R_2^2 - D^2)} \cdot \cos\theta + D \cdot \sin\theta$$

$$Y_2 = \sqrt{(R_2^2 - D^2)} \cdot \sin\theta - D \cdot \cos\theta$$

Lastly, the point  $(X_2, Y_2)$  must be converted to a point  $(X, Y)$  relative to  $(X_1, Y_1)$  which will be the new origin.

$$X = X_2 - X_1$$

$$Y = Y_2 - Y_1$$

Once the data has been converted to this reference origin, it is much easier to automate the calculation of the P(K) for that range and MET comparison.

Prior to generating the data, it was necessary to develop a model that would explain the relation of the radar aim points with the balloon aim points. This is discussed in the next chapter.



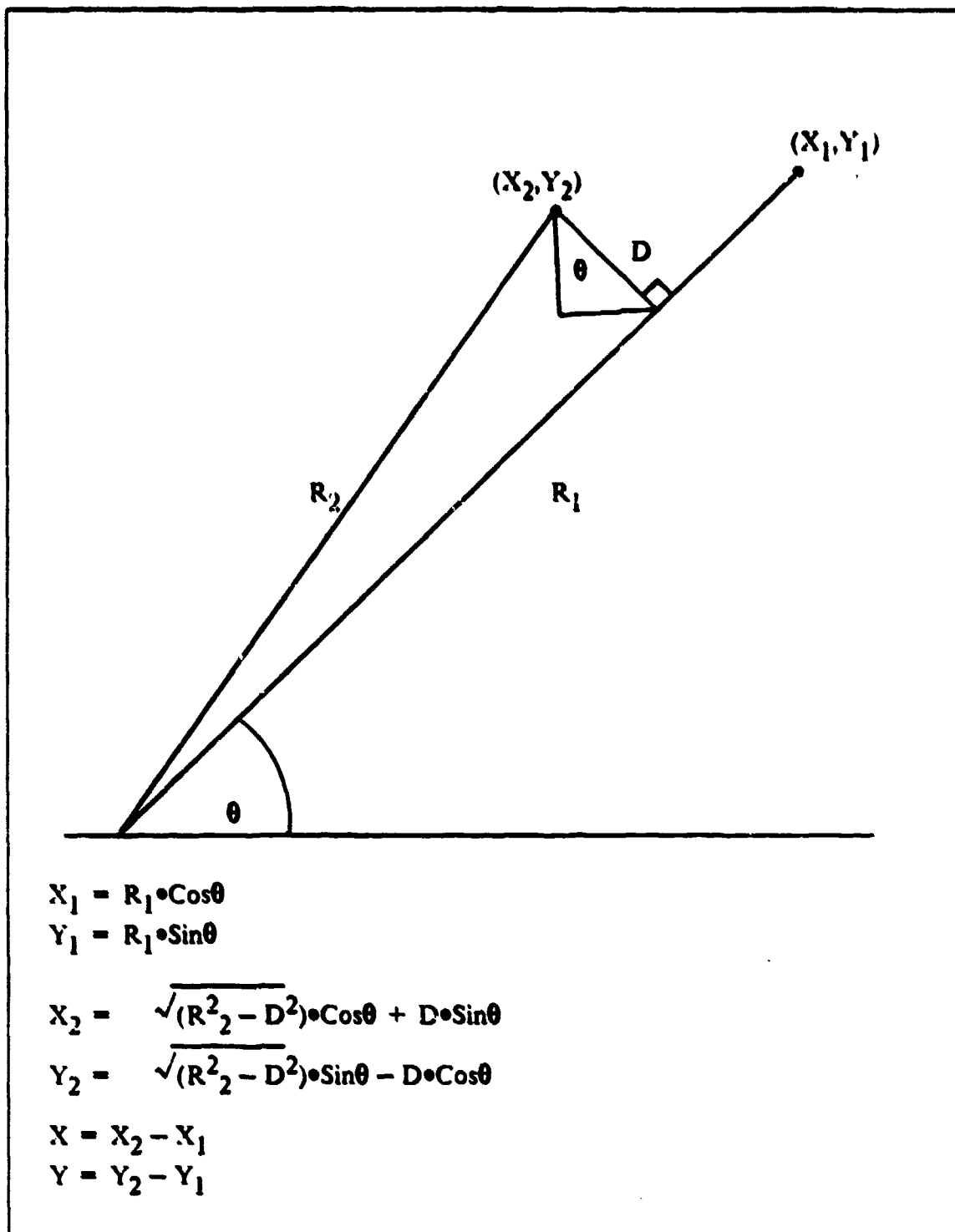


Figure 2.2 Transformation to Reference Origin.

### III. MODEL DEVELOPMENT

With any problem, there is more than one approach which will culminate in a solution. With this problem, the methodology of the analysis is very important. Due to the complete lack of live firings, the limited amount of initial MET data available, and the fact that only this MET data was used to produce the data for the analysis, it was important to choose an approach which would maximize the usefulness of the MET data. This chapter describes the model used in the analysis. The first section defines the problem that the model had to fit. The second section describes the determination of the different elements of the model.

#### A. MODEL

As discussed in Chapter II, the limited amount of data and the method of employing the computer model GTRAJ required an analytic model that could describe the absolute accuracy of the radar MET when what was being measured was the accuracy of the radar MET, relative to the balloon MET.

To construct the analytical model, the target location (T) is assumed to be known. If balloon MET is used, an aim point for the artillery piece is determined. This aim point describes the random vector  $TB$ , see Figure 3.1, from the target to the aim point. Ideally, this aim point should be located at T. However, MET data has random errors associated with it that are approximately constant from shot to shot, hence  $TB$  is a random variable, and B will not normally coincide with T.  $TB$  is distributed about T with some mean,  $\mu_B$ , and variance,  $\sigma_B^2$ . For convenience of calculation,  $TB$  is assumed to be distributed according to a circular normal  $(0, \sigma_B^2)$  distribution. The mean is assumed to be 0, as any consistent error recognized during testing of the system, could be compensated for during calibration of the system. Likewise, if radar MET is used,  $TR$ , another random vector is generated, also distributed about T, such that  $TR \sim N(0, \sigma_R^2)$ .  $TR$  and  $TB$  are independent random variables. There is one additional random variable in the model,  $RB$ .  $RB$  is the difference between  $TR$  and  $TB$ . Since  $RB$  is the difference of two normally distributed random variables, it is also normally distributed, [Ref. 15: p. 267],  $RB \sim N(0, \sigma_{RB}^2)$ , where  $\sigma_{RB}^2 = \sigma_R^2 + \sigma_B^2$ . In this analysis, it is the variances of these random variables that are of the most concern.

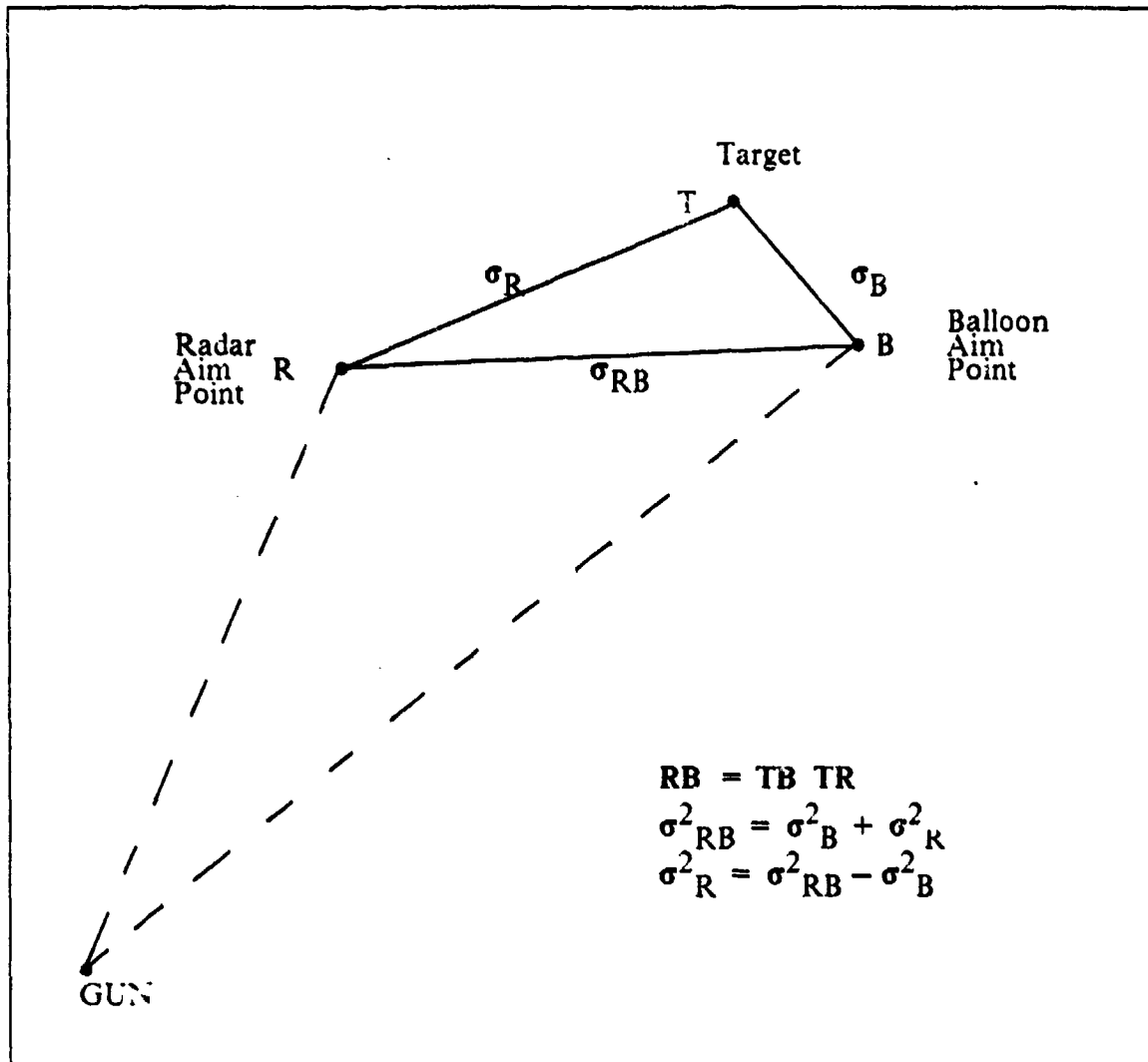


Figure 3.0 Target Location Model.

### B. BIAS DETERMINATION

A measure of  $\sigma^2_{RB}$  is implicitly contained in the output aim points of GTRAJ as it is the radar-to-balloon bias. Consequently, if either  $\sigma^2_B$  or  $\sigma^2_R$  could be calculated or deduced, using the fact that  $\sigma^2_{RB}$  can be estimated with GTRAJ, the third variance could be discovered.

Through many tests and experiments, the US Army has determined the probability of hitting,  $P(h)$ , a target of two different sizes, 10m x 10m and 20m x 20m. These probabilities are specified in FM 6-141-1, [Ref. 8: p. 5-6], and reproduced in part in Table 3.

The probability of hitting a target uniformly distributed across an area A, is given by Equation 3.1. The firing distribution is  $f(x,y)$ .

$$P(h) = \iint_A f(x,y) dx dy \quad (\text{eqn 3.1})$$

If we assume that X is independent of Y,  $f(x,y)$  can be represented as  $f(x) \cdot f(y)$ . Then Equation 3.1 becomes Equation 3.2, where the target is assumed to be centered at the origin and has dimensions of  $2a \times 2b$ .

$$P(h) = \int_{-a}^a f(x) dx \cdot \int_{-b}^b f(y) dy \quad (\text{eqn 3.2})$$

The US Army makes the assumption of bivariate normal firing errors [Ref. 16: p. 13-1], and has published the values of cross-range and down-range ballistic dispersion,  $\sigma_X$  and  $\sigma_Y$ , that have been determined empirically, [Ref. 17: p. A-5]. Table 4 contains an extract of these values. By setting  $P(h)$  equal to the published value for each range, Equation 3.3 and a set of tables for the standard normal distribution, as found in [Ref. 15: p. 580], can be used to iteratively solve for  $\sigma_B$ . Column 4 in Table 3 is the published  $P(h)$ , column 3 is the calculated  $P(h)$  given the inferred value of  $\sigma_B$  listed in column 2.

$$P(h) = \frac{1}{\sqrt{L1}} \int_{-a}^a \exp\left[-\frac{X^2}{2\sigma_1^2}\right] dx \cdot \frac{1}{\sqrt{L2}} \int_{-b}^b \exp\left[-\frac{Y^2}{2\sigma_2^2}\right] dy \quad (\text{eqn 3.3})$$

where  $L1 = 2\pi\sigma_1^2$ ,  $L2 = 2\pi\sigma_2^2$ ,  $\sigma_1^2 = \sigma_X^2 + \sigma_B^2$ , and  $\sigma_2^2 = \sigma_Y^2 + \sigma_B^2$ .

Once  $\sigma_B^2$  has been determined,  $\sigma_{RB}^2$  can be calculated. Knowing  $\sigma_B^2$  and  $\sigma_{RB}^2$ ,  $\sigma_R^2$  is then determined by Equation 3.4.

$$\sigma_R^2 = \sigma_{RB}^2 - \sigma_B^2 \quad (\text{eqn 3.4})$$

**TABLE 3**  
**BALLOON BIAS VS RANGE TO TARGET**

Target Size 10m x 10m			
RANGE	BIAS( $\sigma_B$ )	P(h)	FM 6-141-1 P(h)
10km	14.37	.0505	.051
12km	18.16	.03395	.034
14km	20.38	.0268	.027

Target Size 20m x 20m			
RANGE	BIAS( $\sigma_B$ )	P(h)	FM 6-141-1 P(h)
10km	16.09	.1657	.166
12km	20.01	.1168	.117
14km	22.61	.0928	.093

**TABLE 4**  
**BALLISTIC DISPERSION ESTIMATES FOR 155MM HOWITZER,  
M109A1**

RANGE	$\sigma_X$	$\sigma_Y$
10km	8	39
12km	10	44
14km	13	51

Mathematically, it makes no difference whether the arbitrary origin is located at the target, or if it is at the aim point provided by the balloon MET. Because it is more

convenient in using GTRAJ. the remaining analysis will assume that the balloon MET aim point is the origin, and  $\mathbf{BT}$  is distributed about  $\mathbf{B}$ ;  $\mathbf{BT} \sim \mathcal{N}(0, \sigma^2_{\mathbf{B}})$ .

After selecting the appropriate MOE, which will be discussed in the next chapter, the calculated values of  $\sigma^2_{\mathbf{R}}$  and  $\sigma^2_{\mathbf{B}}$  will be used to generate the data to be analyzed in Chapter VI.

## IV. MOE DETERMINATION

Chuyev [Ref. 18: p. 11], emphasizes that any MOE must be representative of the decision required, be simple in application, and contain, if possible, all of the basic elements under study. In this thesis, two different methods of meteorology data collection are compared. The element of interest is how they individually affect the accuracy of ballistic field artillery, as it impacts on mission accomplishment, when the artillery uses each of the atmospheric models for targeting calculations. As such, the MOE should reflect that interest.

### A. ALTERNATIVES

Ideally, to accurately compare the two MET systems, an experiment should be conducted, where numerous artillery fire missions of all calibers are fired. Such an experiment would be very costly in terms of equipment, ammunition expenditures, and man hours involved in the conduct of the experiment. In such an experiment, the miss distance from the target would be an integral part of the MOE. In this analysis, the distance from the target to the aim point could be considered as a "miss distance." This would be a viable alternative if the firing distribution were circular normal. We want to choose an MOE closely identified with mission accomplishment of field artillery, i.e. destroying the target. Hence, the probability of kill,  $P(k)$ , incorporates artillery "accuracy," as a function of the MET data, (represented by  $\sigma_B$  or  $\sigma_R$ ), in that non-linear formulation most closely associated with mission objective. Hence, the higher the  $P(k)$ , the better the aim point. The approach then is to calculate the  $P(k)$  produced by each system. This approach has intuitive appeal, and it has a closed form solution under the proper assumptions.

### B. CALCULATION OF MOE

Once the MOE has been chosen, it becomes important to determine how to calculate the MOE. Since the radar MET is extrapolated above the planetary boundary layer (PBL), and balloon MET is measured [Ref. 5], the problem is to determine how to remove the effect (bias) of the prevailing winds above the PBL. The method chosen was to "fire" at a target of given range from eight different directions, (N,NE,E,SE,etc.). Therefore, this firing method would have the effect of mitigating the bias if the maximum ordinate of the round was above the PBL.

Assuming each of the eight directions of fire are equally likely, the calculation of the MOE proceeds as follows. Determine each aim point for the eight directions and calculate the  $P(k)$  for each aim point. The  $P(k)$ 's were then averaged to determine a point estimate for the  $P(k)$  for that range, Equation 4.1. This was repeated for each range of interest.

$$P(k)_{\text{range}} = \frac{1}{8} \sum P(k)_{\text{direction}} \quad (\text{eqn 4.1})$$

The comparison  $P(k)$ , which is the average of the range  $P(k)$ 's could be determined in many different ways. The method used should reflect the suspected range distribution of the targets engaged. As such, it could be viewed as a weighted sum of the range  $P(k)$ 's, Equation 4.2, where the weights were assigned based upon the suspected distribution of the ranges. For this analysis, two discrete distributions over 10km, 12km, and 14km were chosen. The weights were the probabilities of the range occurring, see Table 5.

$$P(k) = \sum w_{\text{range}} \cdot P(k)_{\text{range}} \quad (\text{eqn 4.2})$$

RANGE	DIST 1 (p)	DIST 2 (p)
10km	.333	.250
12km	.333	.500
14km	.333	.250

The next chapter presents the detailed calculation of the weighted  $P(k)$ , the MOE selected for the system comparisons. This appears to be the most logical MOE, and is readily calculable.



## V. CALCULATION OF P(K)

When calculating  $P(k)$ , the items of concern are target location, where the weapon is aimed, the firing distribution, and the distribution of the lethal effect of the ordnance being fired at the target. For this analysis, the target was assumed to be a point target located at the origin in the XY plane.

### A. DAMAGE FUNCTION

The probability of destroying a target is the product of the probability of hitting the target,  $P(h)$ , and the conditional probability of killing the target given that it is hit,  $D(r)$ , commonly referred to as the damage function. As explained in Eckler and Burr, [Ref. 19: p. 16], if we assume that a target is located at the origin (0,0) in the XY plane, we can denote the probability density function of weapon impact points by  $f(x,y)$  and the probability of destroying the target if the weapon impacts at  $(x,y)$  by  $D(x,y)$ . Then the unconditional probability of destroying the target with a single round is given by Equation 5.1.

$$P(k) = \iint D(x,y) \cdot f(x,y) dx dy \quad (\text{eqn 5.1})$$

The damage function,  $D(x,y)$  is actually a conditional kill probability. Although not required, in general the damage function is assumed to possess circular symmetry and be non-increasing, [Ref. 13: p. 2]. This means that the damage function is a function of only one variable,  $r = (X^2 + Y^2)^{1/2}$ . Since it is a probability, it ranges from one to zero as  $r$  increases from zero to some maximum lethal radius,  $R$ , away from the target. The damage function represents the probability that  $R$  is greater than  $r$ . As such,

$$D(r) = P(R > r) \quad (\text{eqn 5.2})$$

For this analysis, two damage functions were considered, the so-called cookie cutter weapon and the diffuse Gaussian or Carlton weapon.

### 1. Cookie cutter

Since the damage function is the conditional kill probability, the cookie cutter weapon can be easily visualized as a lethal radius,  $R$ , around the target. This radius is constant and forms a circle around the target, hence the term cookie cutter. If the weapon strikes within this constant radius,  $r \leq R$ , the target will be destroyed, otherwise, the target is undamaged. Conceptually, this weapon has a great deal of appeal. However, as Washburn describes [Ref. 13: pp. 4], when the firing errors are not circular normal, or the aim point is offset from the origin, there is no closed form solution for  $P(k)$ , and numerical integration or other numerical techniques must be employed.

Both of the above situations existed in this analysis, the aim point is not located at the origin and the probability density function for the firing errors, although bivariate normal, was not circular.

### 2. Diffuse Gaussian

The diffuse Gaussian weapon is one of the alternative damage functions that allow a closed form solution under the above conditions. The diffuse Gaussian weapon does not assume that the lethal radius is a constant. Instead,  $r$  is a continuous random variable and has a range of  $(0, \infty)$ . The damage function for the diffuse Gaussian has the form of Equation 5.3 for some scaling factor,  $b$ .

$$D(r) = \exp(-r^2/2b^2) \quad (\text{eqn 5.3})$$

The lethal area for this weapon then becomes  $2\pi b^2$ . During this analysis,  $b$  was chosen such that the weapon lethal area was equal to the lethal area covered by a 155mm high explosive (HE) round that has a bursting radius of 50 meters. Therefore, Equation 5.4 describes the relationship between the damage function and the bursting radius of the 155mm HE round.

$$2\pi b^2 = \pi R^2 \quad (\text{eqn 5.4})$$

Setting  $R$  equal to 50m, and solving for  $b$ , yields  $b = 35.36$ .

## B. FIRING DISTRIBUTION

The US Army has, over the years, conducted numerous tests to determine the firing distribution and its parametric values for the indirect fire weapons in the arsenal. The distribution specified in DARCOM-P 706-101, [Ref. 16: pp. 3-1,A-5], is an elliptical bivariate normal distribution where both the cross-range and down-range components of the ballistic dispersion vary with the range to the target. The firing distribution is shown in Equation 5.5, where  $(X_0, Y_0)$  is the aim point, and  $(X, Y)$  is the actual point of impact, with  $\sigma_X$  and  $\sigma_Y$  the ballistic dispersion.

$$f(x,y) = \frac{1}{2\pi\sigma_X\sigma_Y} \exp\left(-\left[\frac{(X-X_0)^2}{2\sigma_X^2} + \frac{(Y-Y_0)^2}{2\sigma_Y^2}\right]\right) \quad (\text{eqn 5.5})$$

The values for  $\sigma_X$  and  $\sigma_Y$  as found in FM 101-61-5-3, [Ref. 17: p. A-5], are extracted and appear in Table 6.

TABLE 6  
BALLISTIC DISPERSION ESTIMATES FOR 155MM HOWITZER,  
M109A1

RANGE	$\sigma_X$	$\sigma_Y$
10km	8m	39m
12km	10m	44m
14km	13m	51m

## C. DETERMINATION OF P(K)

### 1. Numerical Determination

The assumptions of normal firing errors and the diffuse Gaussian damage function combine very nicely to produce a closed form solution for P(k). Using Equations 5.4 and 5.5 in Equation 5.1, we obtain Equation 5.6. As Washburn, [Ref. 13: p. 5], states, this equation assumes the center of the error distribution is

$(\mu_X, \mu_Y)$  with ballistic dispersion of  $(\sigma_X, \sigma_Y)$ . For this situation, the target is assumed to be located at the origin with certainty.

$$P(k) = \frac{b^2}{\sqrt{(b^2 + \sigma_X^2)(b^2 + \sigma_Y^2)}} \exp\left(-\left[\frac{\mu_X^2}{2(b^2 + \sigma_X^2)} + \frac{\mu_Y^2}{2(b^2 + \sigma_Y^2)}\right]\right) \quad (\text{eqn 5.6})$$

As described in Chapter II, the way GTRAJ was used required one of the MET data sets to be used as a reference during the comparisons. Since the balloon MET was the reference, all of the comparison aim points assumed that the balloon MET aim point was the origin, and the target was a random distance away from the balloon MET aim point. This does not invalidate any of the equations developed so far, but the target bias,  $\sigma_B$ , must be incorporated into Equation 5.6 to produce the probability of killing the target. Thus Equation 5.7 is the probability of killing the target with a single round, where  $(X_0, Y_0)$  is the GTRAJ generated aim point.

$$P(k) = \frac{b^2 \exp\left\{-\left(\frac{X_0^2}{2(b^2 + \sigma_X^2 + \sigma_B^2)} + \frac{Y_0^2}{2(b^2 + \sigma_Y^2 + \sigma_B^2)}\right)\right\}}{(b^2 + \sigma_X^2 + \sigma_B^2)^{1/2} (b^2 + \sigma_Y^2 + \sigma_B^2)^{1/2}} \quad (\text{eqn 5.7})$$

When applying Equation 5.7 to the aim point data, it was necessary to recall that in the case where the radar was being compared against the current balloon,  $\sigma_{RB}^2$  was implicitly contained in the offset aim point. As such, to calculate the absolute  $P(k)$  for the radar MET, it was necessary to subtract out the balloon bias when making the calculations.

## 2. Graphical Determination

Figure 5.1 illustrates a graphical method of determining the radar bias,  $\sigma_R$ , which was used to verify the calculations described above.

The plots represent the change in the arithmetic mean of the  $P(k)$  for each type comparison, as the value of  $\sigma_B$  increases from 0 to 100. The plot of the current balloon (top line) can be thought of as an ideal standard, as for that case, the aim point was the origin and the only errors were due to ballistic dispersion. This is Equation 5.7 with  $X_0 = Y_0 = 0$ , and  $\sigma_B$  varying along the horizontal axis as indicated.

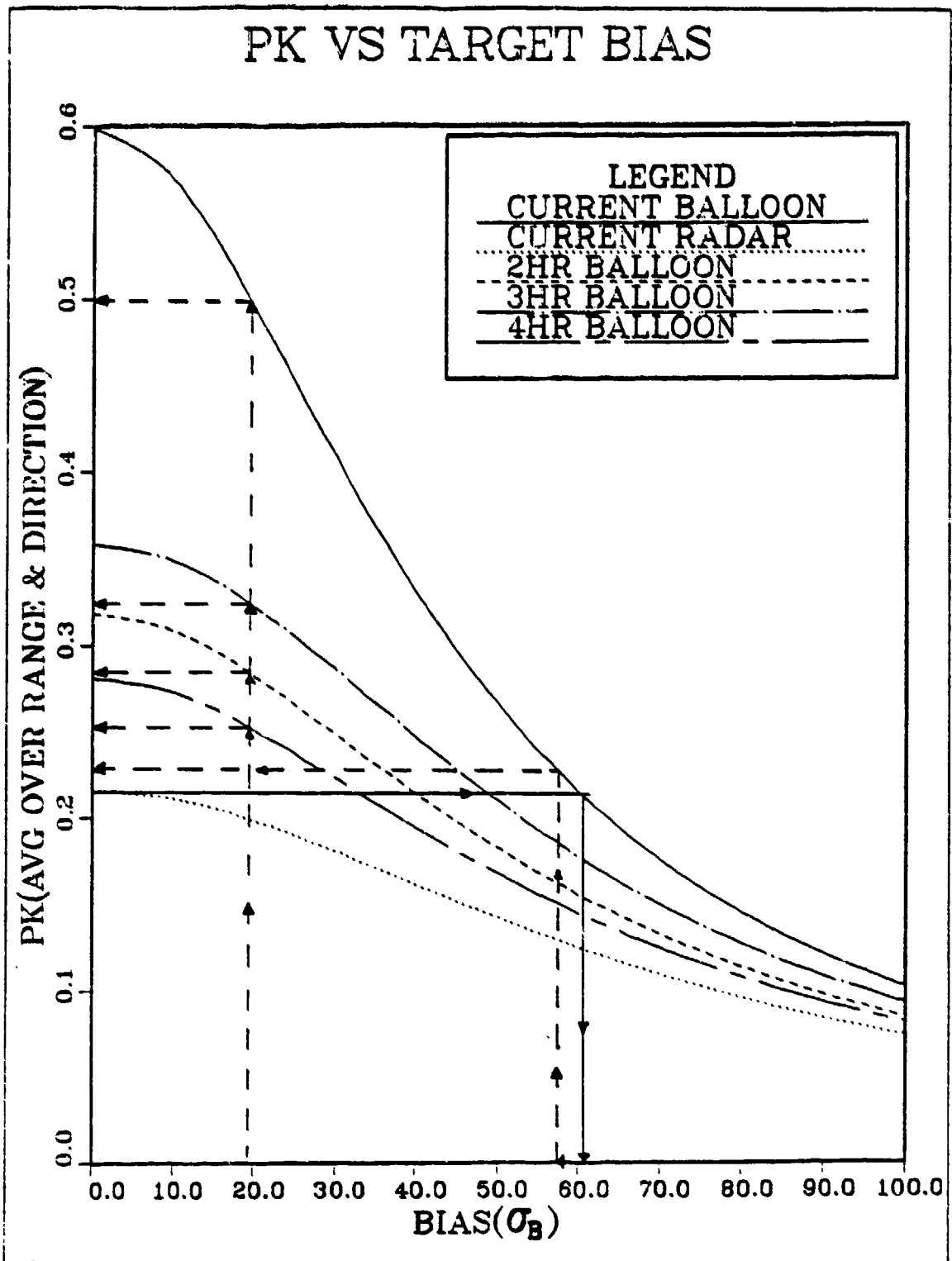


Figure 5.1 Graphical Bias Determination.

To determine the total amount of bias represented by the average radar MET  $P(k)$ , extend a horizontal line from the radar MET curve at the ordinate to intersect with the ideal curve. Then drop a vertical line to the abscissa. The point of intersection is the amount of bias in addition to the ballistic dispersion necessary to achieve that  $P(k)$ . The solid line represents this process on the radar  $P(k)$ .

Since the value of  $\sigma_{RB}$  is represented implicitly in the aim point for the radar MET, it is necessary to subtract the balloon bias  $\sigma_B$  so the  $P(k)$  will reflect the absolute radar accuracy.

The value of the average radar MET  $P(k)$  on Figure 5.1 is .2164. This represents an average bias of approximately 60.5 meters as read from the graph. This bias is the radar to balloon bias  $\sigma_{RB}$ . If we substitute the average  $\sigma_B$  (19.57) represented in Table 3, into Equation 3.4, an average radar bias of approximately 57.25 is calculated. To determine the absolute average radar  $P(k)$ , enter the graph at the bottom with this number (dashed line) and reverse the process described above. This yields an average radar  $P(k)$  of approximately .23.

The remaining four curves on the graph describe balloon MET  $P(k)$ 's at various ages. These curves were calculated assuming  $\sigma_B = 0$ . As such, to reflect the "absolute" balloon MET accuracy, the value of  $\sigma_B$  must be added as in Equation 5.7 to produce accurate balloon MET  $P(k)$ 's. Graphically, enter the graph at  $\sigma_B = 19.57$ , and go up until intersecting each balloon MET  $P(k)$  curve. Then extend a horizontal line to the ordinate to determine the absolute balloon MET  $P(k)$  for each curve. The relative and graphical absolute values of the  $P(k)$ 's are included in Table 7.

TABLE 7  
MET COMPARISON P(K)

COMPARISON	RELATIVE P(k)	ABSOLUTE P(k)
RADAR	.2179	.23
2HR	.3195	.28
3HR	.3547	.33
4HR	.2750	.25

As is apparent from Figure 5.1, when the balloon MET bias was incorporated into the results, the radar MET P(k) got better since the balloon MET was subtracted, and the P(k) provided by the stale balloon MET got worse as the balloon MET bias was added.

Since the individual radar aim points inherently contained the value of  $\sigma_{RB}$ , a way of extracting the effect of  $\sigma_B$ , thereby leaving only the effect of  $\sigma_R$ , was required. Recognizing that the target distribution was circular normal, the length of the vector produced from the origin to the aim point could be *scaled* to reflect the "magnitude" of the radar bias. To accomplish this scaling, each aim point produced in the radar comparisons was transformed as in Equation 5.8

$$(X_0', Y_0') = \sqrt{(\sigma_{RB}^2 - \sigma_B^2)} \cdot \sigma_{RB} \cdot (X_0, Y_0) \quad (\text{eqn 5.8})$$

These new aim points were used in Equation 5.7 to calculate the individual point P(k)'s. These P(k)'s were averaged to produce a P(k) for the given range, and the range P(k)'s were combined as described in Chapter IV to produce the comparison P(k) used in the analysis in the next chapter.

## VI. ANALYSIS OF RESULTS

This chapter is a detailed analysis of the results of the comparisons in Table 1. The analysis is both graphical and statistical. Section 1 is concerned with the graphical analysis, Section 2 follows up with testing of statistical hypothesis. In this chapter, only the data from the two range distributions is considered. The individual range data and some ancillary graphical displays are included in Appendix B.

### A. GRAPHICAL ANALYSIS

The graphical analysis consists of two parts, a review of the data histograms as compared to a normal density function with the results of the Kolmogorov-Smirnov, (K-S), goodness of fit test, [Ref. 20: p. 346], for a normal distribution, and analysis of the empirical quantile - quantile (Q - Q) plots.

As indicated earlier, the first range distribution assumed that a target had an equal probability of being located at either 10km, 12km, or 14km from the gun. The only comparisons considered in this portion of the analysis are those with five or more data points.

As is evident from the histograms in Figures 6.1 - 6.3, the radar MET  $P(k)$  data is the only one which remotely resembles unimodality. None of the histograms suggest similarity of distributions. However, due to the small sample sizes, similarities could not be ruled out. As indicated in Table 8, each of the samples has a rather high level of significance for the K-S test statistic, which indicates a reasonably good fit when compared with a normal distribution, even with these few data points. The radar comparison was the only sample which had enough data points to allow a Chi-Square goodness of fit test to be performed [Ref. 20: p. 189].

As found in Chambers, et al., [Ref. 21: p. 68], the empirical Q - Q plot can be used to determine if the two data sets differ by an additive or multiplicative constant. The points plotted in Figures 6.4 and 6.5 are the values of  $P(k)$  associated with every fifth quantile, (e.g. 5, 10, 15, ..., 95), of each data set. Each set of quantiles was calculated based upon the individual sample, i.e. given the sample, the 5th, 10th, etc. quantile was determined. The quantiles for the two hour or four hour balloon MET were then plotted against the radar MET quantiles. As seen in Figure 6.4, the majority of the plotted values lie above the  $X = Y$  line (solid line). A line parallel to that line



**TABLE 8**  
**GOODNESS OF FIT TEST SIGNIFICANCE LEVELS**

Comparison	Sample Size	K-S Test	X <sup>2</sup> Test
RANGE DISTRIBUTION #1			
RADAR	19	.541	.614
2HR	9	.786	---
4HR	5	.566	---
RANGE DISTRIBUTION #2			
RADAR	19	.829	.344
2HR	9	.743	---
4HR	5	.565	---

(dashed line) can be drawn such that approximately half of the data points are on either side of it. The dashed line represents a shifting of the X=Y line by approximately .05 units. This indicates that on the average, the two hour MET P(k)'s are approximately .05 higher in value than the radar MET P(k)'s. In Figure 6.5 it is possible to construct a line shifted by approximately .02 units. Thus, the four hour P(k) have a value that is approximately .02 higher than the radar MET P(k). As is shown in the next section, this is not necessarily statistically significant.

## B. STATISTICAL TESTING

Although all of the data sets had high K-S significance levels for a normal distribution, two transforms suggested by Bartlett, [Ref. 22: p.52], were applied against them; the so called *Fisher's Z transform* where  $Z = 1/2 \ln[(1+p)/(1-p)]$ , and the arcsin transform where  $Z = \arcsin(\sqrt{p})$ . Assuming that the goal was to spread the data and stabilize the variance, a change of variable was imposed where  $r = 1-2p$ , then the *Fisher's Z transform* was used on r. This yielded  $Z = 1/2 \ln[(1-p)/p]$ . But since it was more appealing to have large values of p map into large values of Z, and likewise for small values of p, the reciprocal,  $Z = 2 \ln[p/(1-p)]$ , was chosen. None of these transforms produced any increase in the K-S significance levels.

The objective was to determine if the radar MET could augment the balloon MET, not replace it. Because the much lower cost of developing, testing, and fielding

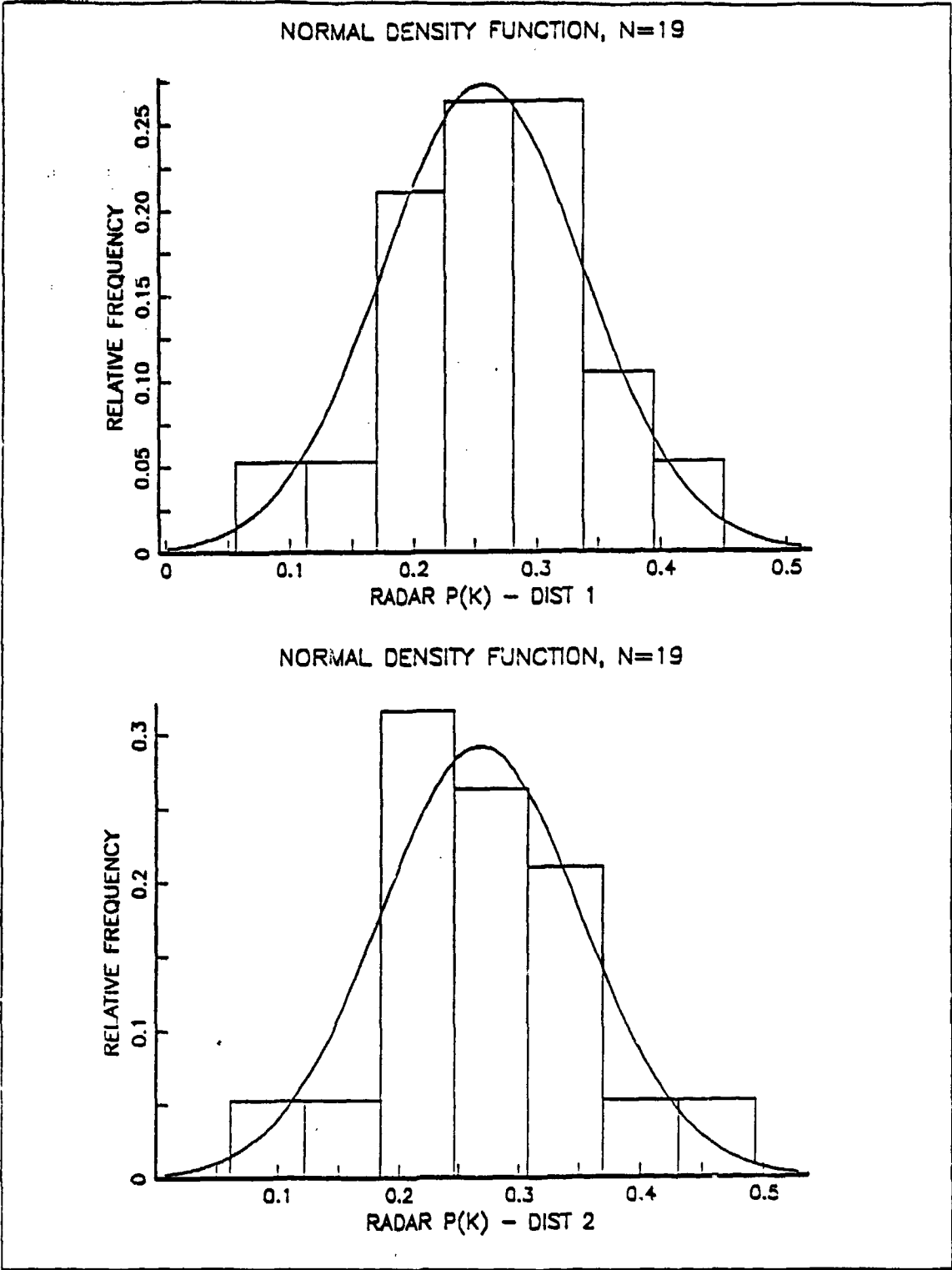


Figure 6.1 Histograms of Radar P(k).

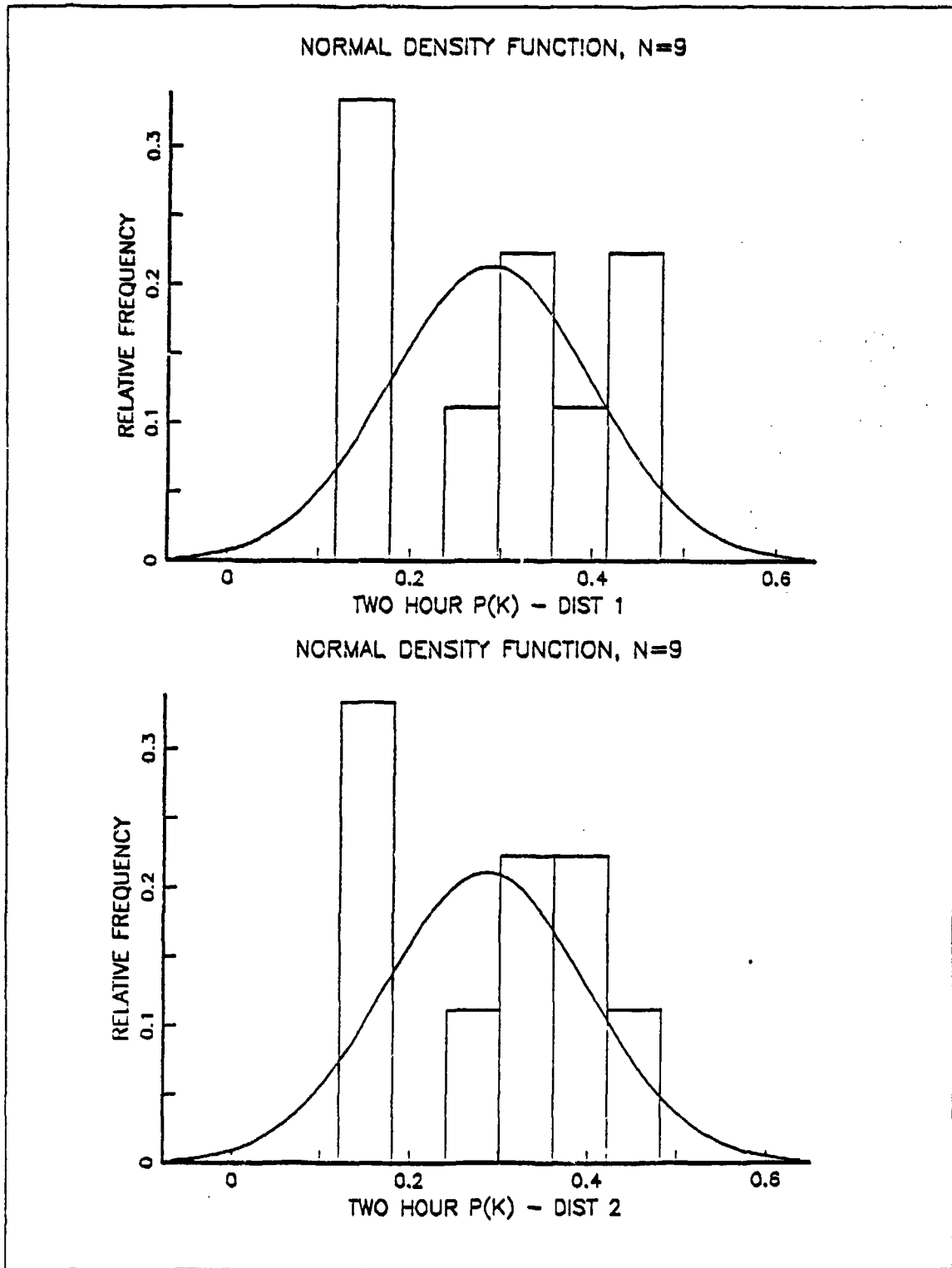


Figure 6.2 Histograms of Two Hour Balloon P(k).

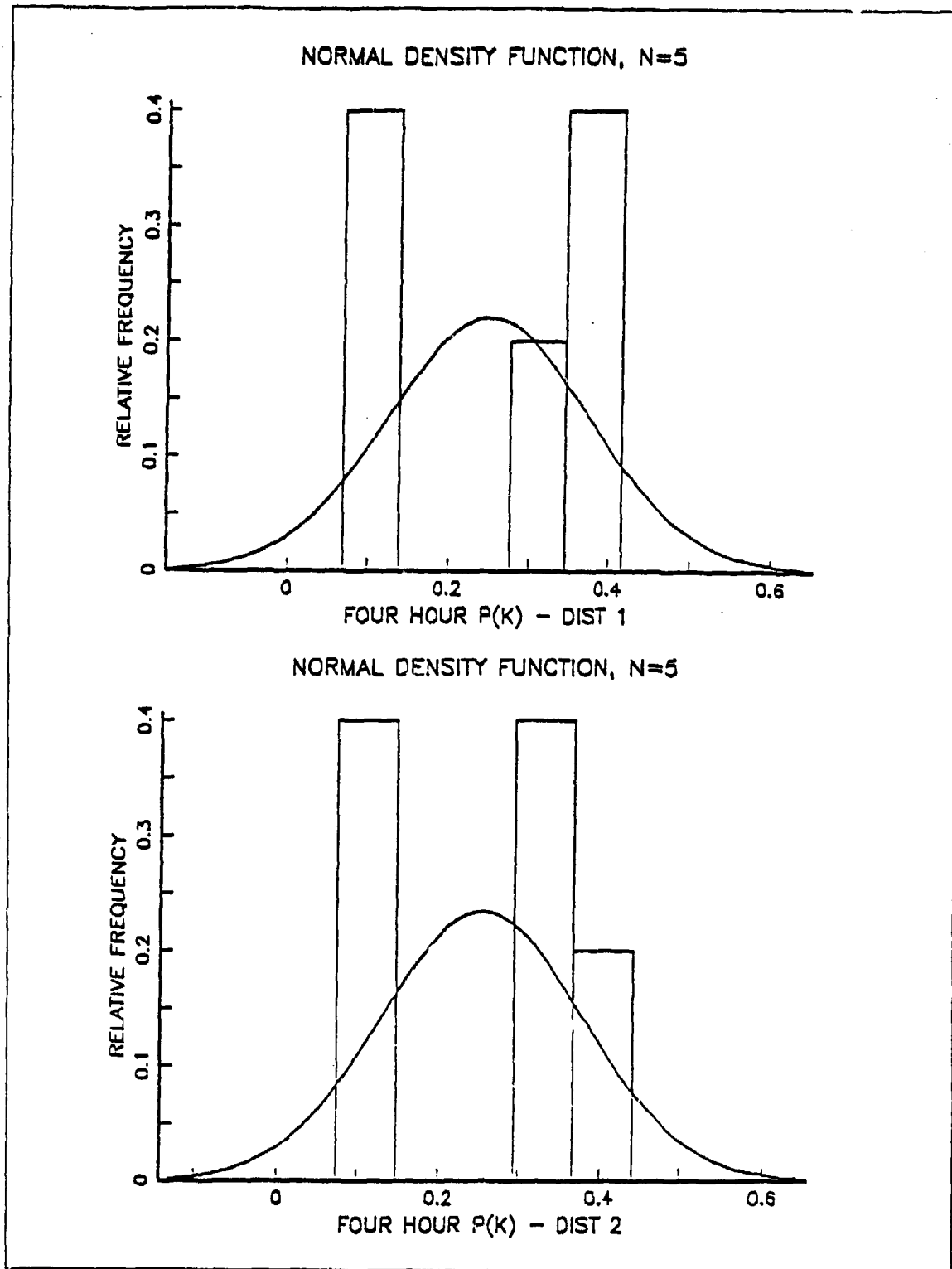


Figure 6.3 Histograms of Four Hour Balloon P(k).

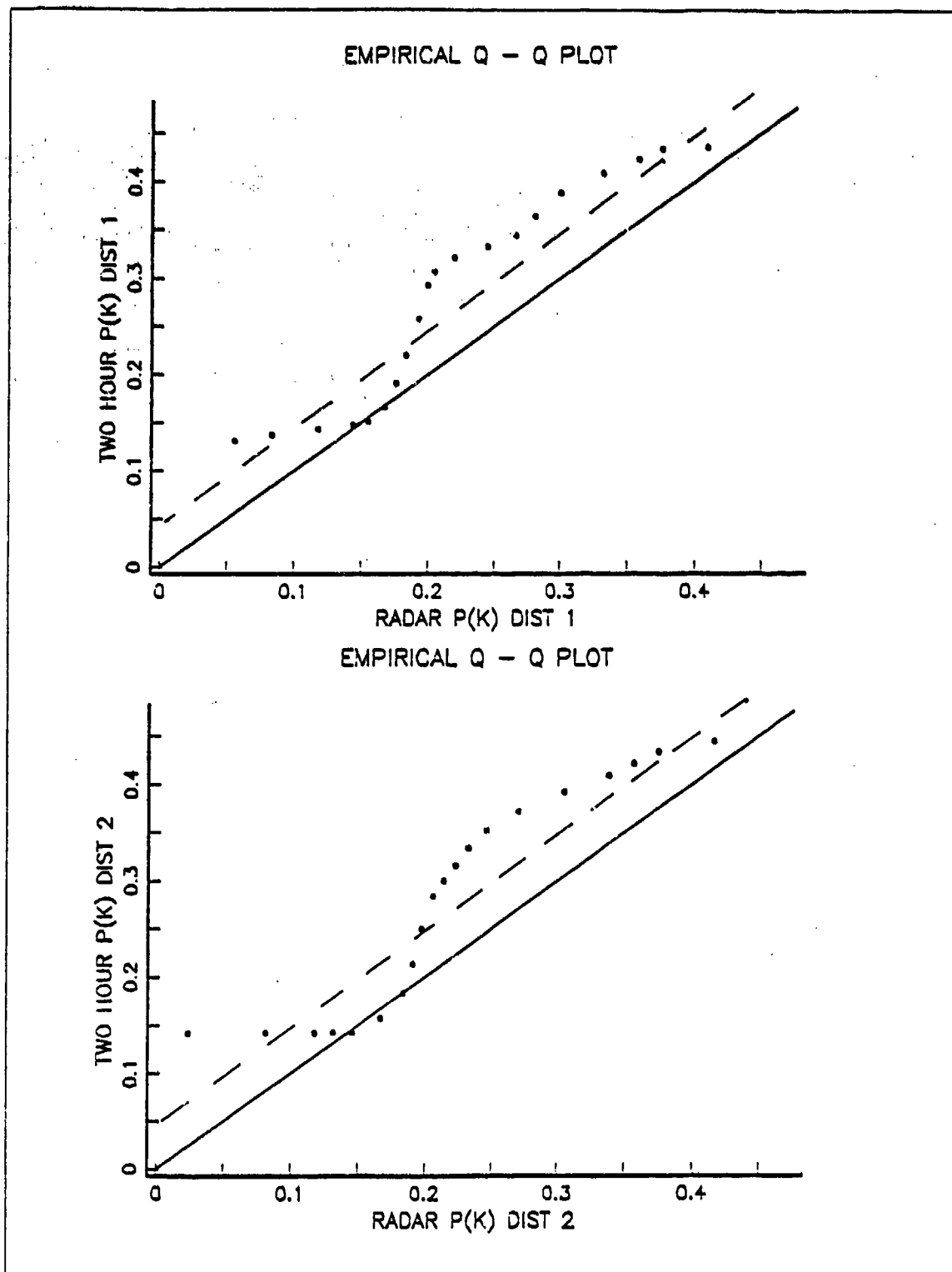


Figure 6.4 Q - Q Plots Radar P(k) Quantiles vs Two Hour P(k) Quantiles.

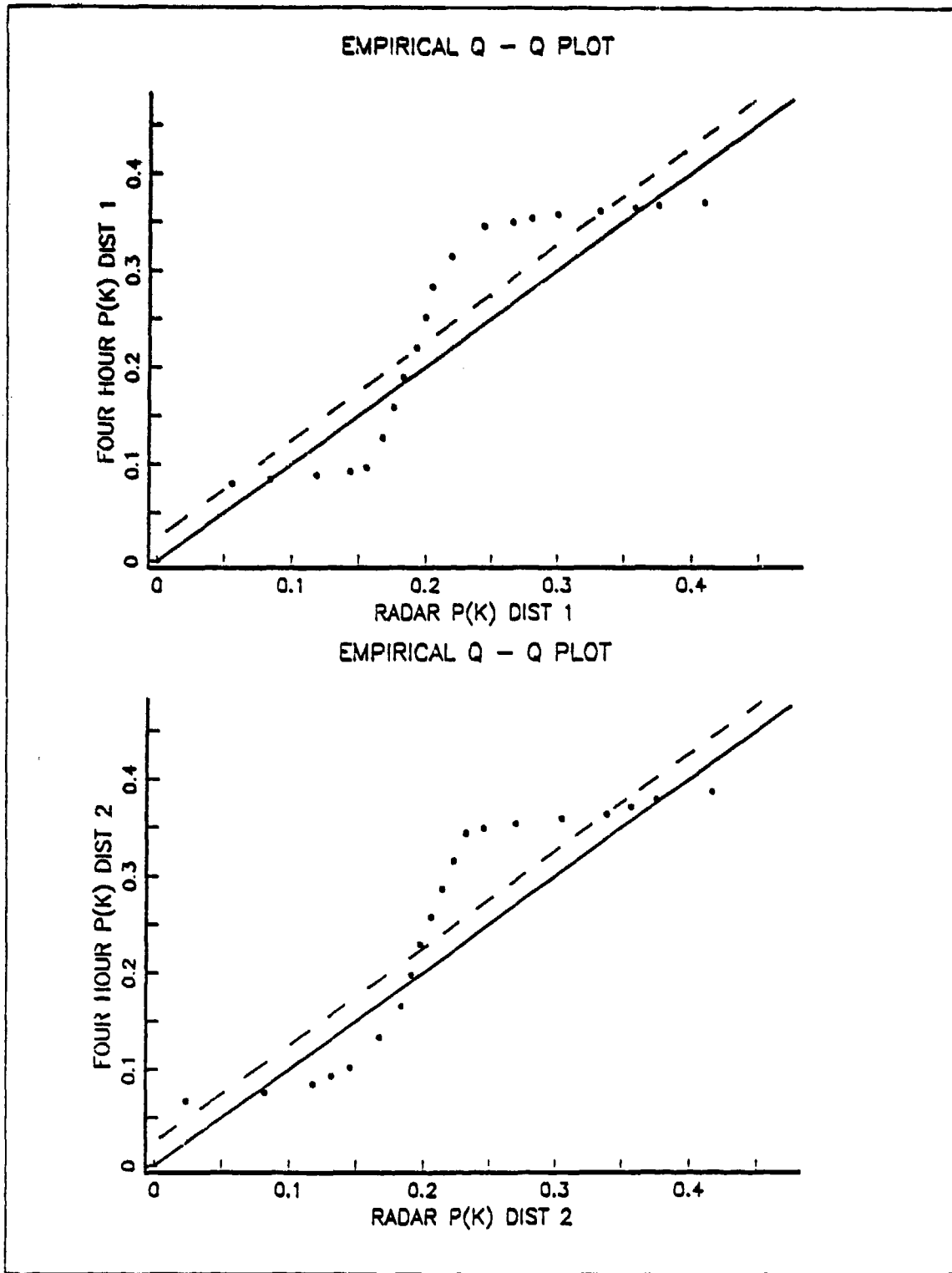


Figure 6.5 Q - Q Plots Radar P(k) Quantiles vs Four Hour P(k) Quantiles.

the radar's software compared with the alternative of procuring additional balloon MDS units was sufficient reason to choose the radar, so long as using the radar resulted in performance *no worse than* the alternative, the hypothesis to be tested was chosen to be:

$H_0$ : Radar MET is at least as good as stale balloon MET

with an alternative of

$H_1$ : Radar MET is not as good as stale balloon MET

This translates into numerical symbology as:

$H_0$ : Radar MET  $P(k) \geq$  stale balloon MET  $P(k)$

$H_1$ : Radar MET  $P(k) <$  stale balloon MET  $P(k)$

It was apparent that as the data sets got larger, the more closely they fit a normal distribution. Although the data sets "fit" a normal distribution, there was some hesitancy to apply the two sample t-test with impunity due to the small sample sizes. As such, in the interest of conservative estimates, both parametric and non-parametric tests were performed. The data produced by the comparisons listed in Table 1 are shown in Table 9, the results for the individual ranges are in Appendix B. This data was tested using the two sample t-test with Welch's approximation to the Behrens-Fisher problem of unequal variances, [Ref. 15: p. 451], and the Mann-Whitney test, [Ref. 20: p. 216] to determine if the data came from the same population. The Mann-Whitney non-parametric test was chosen because it does not assume that the data sets come from any underlying distribution, whereas the two sample t-test assumes that the underlying population is normally distributed. The results of those tests are summarized in Tables 10 and 11. Both tests were performed using MINITAB, a commercially available computer statistical analysis package.

As is evident from the tables, neither of the tests resulted in rejection of the null hypothesis and acceptance of the alternative hypothesis. As such it can not be concluded that the  $P(k)$  provided by the radar MET is any worse than the  $P(k)$  provided by the stale balloon MET. There was some hesitancy in testing the 5hr, 6hr, 7hr, and 9hr data individually, since they each had only two data points, however, by combining them into one data set, a test for balloon data over four hours old was conducted. This is the last line in each distribution in the table. The value of  $\alpha'$  is the level of significance that would have to be used in order to reject the null hypothesis.

**TABLE 9**  
**CALCULATED P(K) FOR MET COMPARISONS**

**RANGE DISTRIBUTION #1**

<b>RADAR</b>	<b>2HR</b>	<b>3HR</b>	<b>4HR</b>
0.128653	0.324017	0.402227	0.335361
0.230605	0.431937	0.329411	0.366009
0.200316	0.137741	0.240176	0.104445
0.214326	0.154158		0.355084
0.202715	0.260526		0.088162
0.078026	0.434561		
0.383268	0.371400		
0.416028	0.151713		
0.225861	0.320409		
0.284265			
0.333147			
0.226094			
0.314591			
0.353041			
0.234335			
0.231733			
0.284585			
0.201747			
0.326326			
	<b>5HR</b>	<b>6HR</b>	<b>7HR</b>
	0.165510	0.261177	0.347922
	0.219295	0.271608	0.170280
			<b>9HR</b>
			0.227994
			0.255972

**RANGE DISTRIBUTION #2**

<b>RADAR</b>	<b>2HR</b>	<b>3HR</b>	<b>4HR</b>
0.152221	0.329131	0.413275	0.347947
0.244974	0.443103	0.312054	0.378912
0.228899	0.143320	0.253295	0.118954
0.241750	0.141840		0.339423
0.195385	0.258664		0.084505
0.063498	0.418551		
0.397695	0.387630		
0.432849	0.142364		
0.251622	0.305028		
0.268500			
0.345476			
0.223661			
0.333423			
0.359733			
0.258948			
0.253771			
0.276574			
0.225085			
0.334287			
	<b>5HR</b>	<b>6HR</b>	<b>7HR</b>
	0.150983	0.251506	0.332766
	0.195812	0.296838	0.151890
			<b>9HR</b>
			0.219481
			0.285708



**TABLE 10**  
**TWO SAMPLE t TEST RESULTS**

**RANGE DISTRIBUTION #1**

Comparison	Reject (Yes/No)	$\alpha'$
Radar vs 2hr balloon	//o	.25
Radar vs 3hr balloon	//oo	.16
Radar vs 4hr balloon	//ooo	.54
Radar vs 5hr balloon	//oooo	.90
Radar vs 6hr balloon	//ooooo	.31
Radar vs 7hr balloon	//ooooo	.49
Radar vs 9hr balloon	//ooooo	.72
Radar vs > 4hr balloon	//oooo	.71

**RANGE DISTRIBUTION #2**

Comparison	Reject (Yes/No)	$\alpha'$
Radar vs 2hr balloon	//o	.35
Radar vs 3hr balloon	//oo	.18
Radar vs 4hr balloon	//ooo	.58
Radar vs 5hr balloon	//oooo	.97
Radar vs 6hr balloon	//ooooo	.42
Radar vs 7hr balloon	//ooooo	.59
Radar vs 9hr balloon	//ooooo	.62
Radar vs > 4hr balloon	//oooo	.84

Additionally, similar tests were conducted on data produced by appending current radar wind values to 2hr and 4hr stale balloon atmospheres (temperature and pressure). This data was then tested against the 2hr and 4hr stale balloon MET P(k)'s. These tests were to determine if the composite two or four hour data sets were as good as the two or four stale balloon data sets. In both cases, rejection of the null hypothesis that the composite data set was as good as the stale data set and acceptance of the alternative hypothesis was not possible, with exceptionally high  $\alpha'$  values required to reject.

TABLE 11  
MANN-WHITNEY TEST RESULTS

RANGE DISTRIBUTION #1

Comparison	Reject $H_0$ (Yes/No)	$\alpha'$
Radar vs 2hr balloon	///o	.2455
Radar vs 3hr balloon	///oo	.0756
Radar vs 4hr balloon	///ooo	.3881
Radar vs 5hr balloon	///oooo	.8467
Radar vs 6hr balloon	///ooooo	.3823
Radar vs 7hr balloon	///ooooo	.5370
Radar vs 9hr balloon	///oooo	.5000
Radar vs > 4hr balloon	///oo	.6837

RANGE DISTRIBUTION #2

Comparison	Reject $H_0$ (Yes/No)	$\alpha'$
Radar vs 2hr balloon	///o	.3653
Radar vs 3hr balloon	///oo	.1463
Radar vs 4hr balloon	///ooo	.4435
Radar vs 5hr balloon	///oooo	.9181
Radar vs 6hr balloon	///ooooo	.4287
Radar vs 7hr balloon	///ooooo	.6790
Radar vs 9hr balloon	///oooo	.6099
Radar vs > 4hr balloon	///oo	.8676

Conover's normal approximation, [Ref. 20: p. 217], was used for  $\alpha' > .5000$

## VII. CONCLUSIONS AND RECOMMENDATIONS

### A. CONCLUSIONS

The original data was very sparse and not gathered with this analysis in mind. Hence, the results are not as conclusive as an experiment designed for that purpose could show. However, the objective of this thesis was to evaluate the results of a "pilot study" to determine if it was advisable to proceed with further testing and development of the WINDFINDER capabilities. The results of this analysis do in fact strongly support further testing and development. The large level of significance necessary to reject the null hypothesis in all comparisons for both distributions considered shows that not only can it not be concluded that the radar MET P(k) is worse than the stale balloon MET P(k), but there appears to be some evidence that the radar MET P(k) is as good as the stale balloon MET P(k). If this capability were available to the artillery units in the field during combat, it is conceivable that there would be a significant increase in the accuracy of first round artillery shots under rapidly changing weather conditions.

This capability does not come for free. By using the FIREFINDER radar in the WINDFINDER mode, an increase in the electromagnetic radiating time is incurred. This increase in radiating time would most likely result in some increase in the radar vulnerability, which could degrade the performance of the radar in its counter-battery mission. This issue of increased vulnerability versus increased first round accuracy during severe climatological conditions is of paramount concern to the artillery community as a whole. However, it is beyond the scope of this thesis, and is mentioned here only in the interest of completeness.

### B. RECOMMENDATIONS

Given such strong indications of parity between the two MET systems, the next and most logical, phase of testing should be pursued. These results warrant the expense of a specially designed and administered field experiment where both MET systems are employed and targets are engaged by artillery of all calibers under as varied conditions as possible. This experiment should include normal, adverse, and rapidly changing weather conditions, and be conducted during all times of the day and night, for it is then that the true strengths and weaknesses of both systems could be evaluated.

## APPENDIX A COMPUTER MET MESSAGES

This appendix contains two computer MET messages. They are the data gathered by ASL on 28 February 1986 at 0500hrs. The first message is the balloon MET data, the second is the radar MET data.

The columns are:

- Altitude zone - these are explained in FM 6-15, [Ref. 4]
- Direction the wind is coming from in mils x .1, i.e. 710 mils is listed as 71.0
- Wind speed in knots
- Temperature in °K x 10.0, i.e. 290.3 is listed as 2903.0
- Barometric Pressure in millibars

Since the radar is not effective in sensing the wind signature above the planetary boundary layer (PBL), the wind values above the PBL must be estimated. The method used to estimate these values is to assume that they remain constant above the highest zone that the radar can sense, and set them equal to the values in the highest zone sensed. The analytic atmosphere estimates temperature and pressure values within each zone, and is not limited by the PBL.

The dates and times that MET data was gathered at Yuma are listed below.

28 February 1986	4 March 1986
0500hrs	0500hrs
0800hrs	0800hrs
1400hrs	1000hrs
1 March 1986	1200hrs
0800hrs	1400hrs
1000hrs	7 March 1986
1200hrs	1400hrs
1400hrs	8 March 1986
3 March 1986	0800hrs
0500hrs	1000hrs
0800hrs	1200hrs
1000hrs	
1200hrs	
1400hrs	

## BALLOON DATA

0.0	71.0	4.0	2903.0	996.0
1.0	182.0	5.0	2966.0	984.0
2.0	184.0	12.0	2989.0	956.0
3.0	179.0	9.0	2955.0	913.0
4.0	219.0	8.0	2928.0	862.0
5.0	242.0	11.0	2855.0	813.0
6.0	303.0	11.0	2854.0	766.0
7.0	328.0	13.0	2854.0	721.0
8.0	301.0	9.0	2768.0	679.0
9.0	319.0	4.0	2716.0	638.0
10.0	378.0	7.0	2704.0	599.0
11.0	356.0	8.0	2667.0	562.0
12.0	307.0	8.0	2621.0	510.0
13.0	233.0	13.0	2547.0	447.0
14.0	190.0	16.0	2445.0	390.0
15.0	181.0	11.0	2385.0	339.0
16.0	201.0	13.0	2281.0	293.0
17.0	174.0	10.0	2228.0	252.0
18.0	555.0	6.0	2198.0	216.0
19.0	570.0	23.0	2166.0	185.0
20.0	552.0	22.0	2156.0	158.0
21.0	552.0	22.0	2156.0	158.0
22.0	552.0	22.0	2156.0	158.0
23.0	552.0	22.0	2156.0	158.0
24.0	552.0	22.0	2156.0	158.0
25.0	552.0	22.0	2156.0	158.0
26.0	552.0	22.0	2156.0	158.0

## RADAR DATA

0.0	71.0	4.0	2904.0	996.0
1.0	101.0	6.0	2905.0	984.0
2.0	146.0	10.0	2897.0	956.0
3.0	220.0	17.0	2884.0	912.0
4.0	173.0	16.0	2867.0	859.0
5.0	153.0	17.0	2850.0	809.0
6.0	202.0	22.0	2824.0	762.0
7.0	161.0	15.0	2790.0	717.0
8.0	214.0	15.0	2756.0	674.0
9.0	212.0	10.0	2723.0	633.0
10.0	268.0	12.0	2689.0	595.0
11.0	268.0	12.0	2656.0	558.0
12.0	268.0	12.0	2607.0	506.0
13.0	268.0	12.0	2541.0	443.0
14.0	268.0	12.0	2475.0	387.0
15.0	268.0	12.0	2410.0	336.0
16.0	268.0	12.0	2345.0	291.0
17.0	268.0	12.0	2279.0	251.0
18.0	268.0	12.0	2214.0	216.0
19.0	268.0	12.0	2167.0	185.0
20.0	268.0	12.0	2141.0	158.0
21.0	268.0	12.0	2115.0	134.0
22.0	268.0	12.0	2089.0	114.0
23.0	268.0	12.0	2062.0	97.0
24.0	268.0	12.0	2048.0	82.0
25.0	268.0	12.0	2058.0	69.0
26.0	268.0	12.0	2083.0	59.0

## APPENDIX B INDIVIDUAL RANGE P(K) RESULTS

This appendix is a listing of the calculated P(k)'s for the individual ranges. The first column is for 10km, the second for 12km, and the third column contains the results for 14km. The data are divided by the type of comparison indicated.

### CURRENT BALLOON

0.5725954	0.4988983	0.4307786
-----------	-----------	-----------

### RADAR

0.1503655	0.2229242	0.0126696
0.2019216	0.2880815	0.2018108
0.0992097	0.3146486	0.1870896
0.1778179	0.3360222	0.1291387
0.3447584	0.1733936	0.0899942
0.2108652	0.0199147	0.0032994
0.4589084	0.4409747	0.2499223
0.4599515	0.4833126	0.3048186
0.3384876	0.3289025	0.0101937
0.4213747	0.2212076	0.2102124
0.3436825	0.3824658	0.2732918
0.2359142	0.2163641	0.2260036
0.4019745	0.3899185	0.1518801
0.4160435	0.3798121	0.2632663
0.3091222	0.3327846	0.0610993
0.2146326	0.3198849	0.1606818
0.3300768	0.2525410	0.2711387
0.1868073	0.2950965	0.1233388
§ 0.5539195	0.3581699	0.0668874

### 2 HOUR OLD BALLOON

0.5209001	0.3444750	0.1066748
0.5125056	0.4766012	0.3067035
0.2345792	0.1600578	0.0185848
0.2911931	0.1048861	0.0663935

0.2302094	0.2530764	0.2982931
0.5553990	0.3705214	0.3777641
0.4383873	0.4363207	0.2394931
0.2705291	0.1143149	0.0702957
0.4702870	0.2588881	0.2320506

**3 HOUR OLD BALLOON**

0.5004889	0.4464195	0.2597735
0.4837357	0.2599821	0.2445163
0.2800654	0.2926543	0.1478076

**4 HOUR OLD BALLOON**

0.4455863	0.3857059	0.1747917
0.5199641	0.4176212	0.1604406
0.0491037	0.1624793	0.1017524
0.4573408	0.2924389	0.3154725
0.1584195	0.0735352	0.0325306

**5 HOUR OLD BALLOON**

0.3017880	0.1074039	0.0873375
0.2954184	0.1253636	0.2371041

**6 HOUR OLD BALLOON**

0.2988767	0.2224923	0.2621628
0.2775682	0.3725309	0.1647241

**7 HOUR OLD BALLOON**

0.5555493	0.2872987	0.2009179
0.2116547	0.0967200	0.2024645

**9 HOUR OLD BALLOON**

0.3636018	0.1939395	0.1264418
0.2751556	0.3749167	0.1178429

## LIST OF REFERENCES

1. Chadwick, R.B., Moran, K.P., Morrison, G.E., and Campbell, W.C., *Measurements Showing the Feasibility for Radar Detection of Hazardous Wind Shear at Airports*, AFGL-TR-78-0160, Final Report, National Oceanic and Atmospheric Administration (NOAA), Boulder, Colorado, 1 November 1976 - 28 February 1978.
2. Zrnica, Dusan S., Smith, Steven D., Witt, Arthur, Rabin, Robert M., and Sachidananda, Mangolare, *Wind Profiling With Microwave Radars of Stormy and Quiescent Atmospheres*, NOAA Technical Memorandum ERL NSSL-98, National Severe Storms Laboratory, Norman, Oklahoma, February 1986
3. Strauch, R.G., Frisch, A.S., Kropfli, R.A., and Weber, B.L., *A Feasibility Study On the Use of Firefinder Radar for Wind Profiling*, NOAA Technical Memorandum ERL WPL-128, Wave Propagation Laboratory, Boulder, Colorado, December 1985
4. US Army Field Manual FM 6-15, with changes 1 & 2, *Field Artillery Meteorology*, Headquarters, Department of the Army, Washington, D.C., 30 August 1978
5. Numerous telephone conversations between Dr. J. Martin, Atmospheric Sciences Laboratory, White Sands Missile Range, New Mexico, and the author, March 1986 - March 1987
6. Hopfer, Allen G., and Blanco, Abel J., *Boundary Layer Enhancement to Tropospheric Temperature and Pressure Extrapolation Modal*, Atmospheric Sciences Laboratory, White Sands Missile Range, New Mexico, August 1986
7. Numerous telephone conversations between Mr. A. Hopfer, Atmospheric Sciences Laboratory, White Sands Missile Range, New Mexico, and the author, May 1986 - August 1986
8. US Army Field Manual FM 6-141-1, *Field Artillery Target Analysis and Weapons Employment: Nonnuclear*, Headquarters, Department of the Army, Washington, D.C., 15 February 1978
9. Rockower, Edward B., *Notes On Measures Of Effectiveness*, Naval Postgraduate School, Monterey, California, 93943, 19 August, 1985
10. Numerous telephone conversations between John Miller, Ballistic Research Laboratory, Aberdeen, Maryland, and the author, July 1986 - March 1987
11. "General Trajectory Program," (computer source code), Ballistic Research Laboratory, Aberdeen Proving Ground, Maryland
12. Numerous telephone conversations between Dr. D. Snider, Atmospheric Sciences Laboratory, White Sands Missile Range, New Mexico, and the author, December 1985 - March 1987



13. Washburn, Alan, *Notes on Firing Theory*, Naval Postgraduate School, Monterey, California, 93943, 1983
14. Thomas, George B. Jr. and Finney, Ross L., *Calculus and Analytic Geometry*, 6th ed, Addison Wesley Publishing Company, Reading, Massachusetts, May 1984
15. Larson, Harold J., *Introduction to Probability Theory and Statistical Inference*, 3rd ed., J. Wiley, New York, 1982
16. DARCOM PAMPHLET, DARCOM-P 706-101, *Engineering Design Handbook, Army Weapon Systems Analysis, Part One*, US Army Material Development and Readiness Command, Washington, D.C., November 1977
17. US Army Field Manual, FM 101-61-5-3, *Joint Munitions Effectiveness Manual (Surface-to-Surface), Indirect Fire Accuracy, Volume III*, Headquarters, Department of the Army, Washington, D.C., 1980
18. Chuvev, Y. V., *Research of Military Operations*, Military Publishing House, Moscow, USSR, 1970
19. Eckler, A. Ross and Burr, Stefan A., *Mathematical Models of Target Coverage and Missile Allocation*, Military Operations Research Society, 1972
20. Conover, W. J., *Practical Nonparametric Statistics*, J. Wiley, New York, 1980
21. Chambers, John M., Cleveland, William S., Kliener, Beat, and Tukey, Paul A., *Graphical Methods for Data Analysis*, Wadsworth International Group, Belmont, California, 1983
22. Bartlett, M. S., "The Use of Transformations", *Biometrics* Vol 3, 1947, 39-52.

## INITIAL DISTRIBUTION LIST

		No. Copies
1.	Defense Technical Information Center Cameron Station Alexandria, Virginia 22304-6145	2
2.	Library, Code 0142 Naval Postgraduate School Monterey, California 93943-5002	2
3.	Prof. Edward B. Rockower, Code 55Rf Department of Operations Research Naval Postgraduate School Monterey, California 93943-5000	2
4.	LTC F. Marchman Perry, Code 55Pj Department of Operations Research Naval Postgraduate School Monterey, California 93943-5000	2
5.	MAJ David Tyner 11 Maple Avenue Avoca, New York 14809	1
6.	MAJ Gary L. Sipe 5317 Weymouth Dr. Springfield, Virginia 22151	5
7.	Commander Director US Army Atmospheric Sciences Laboratory ATTN: SLCAS-AE-E (J. MARTIN) White Sands Missile Range, New Mexico, 88002-5501	10
8.	Commander Foreign Science and Technology Center ATTN: AIFREA (Steve Eitelman) 220 7th ST NE Charlottesville, Virginia 22901	1